

Tectonics and Magmatism of Ultraslow Spreading Ridges

E. P. Dubinin^a, A. V. Kokhan^a, and N. M. Sushchevskaya^b

^a *Museum of Natural History, Moscow State University, Moscow, 119991 Russia*

e-mail: edubinin08@rambler.ru

^b *Vernadsky Institute of Geochemistry and Analytical Chemistry, Russian Academy of Sciences,
ul. Kosygina 19, Moscow, 119991 Russia*

Received November 26, 2012

Abstract—The tectonics, structure-forming processes, and magmatism in rift zones of ultraslow spreading ridges are exemplified in the Reykjanes, Kolbeinsey, Mohns, Knipovich, Gakkel, and Southwest Indian ridges. The thermal state of the mantle, the thickness of the brittle lithospheric layer, and spreading obliquity are the most important factors that control the structural pattern of rift zones. For the Reykjanes and Kolbeinsey ridges, the following are crucial factors: variations in the crust thickness; relationships between the thicknesses of its brittle and ductile layers; width of the rift zone; increase in intensity of magma supply approaching the Iceland thermal anomaly; and spreading obliquity. For the Knipovich Ridge, these are its localization in the transitional zone between the Gakkel and Mohns ridges under conditions of shear and tensile stresses and multiple rearrangements of spreading; nonorthogonal spreading; and structural and compositional barrier of thick continental lithosphere at the Barents Sea shelf and Spitsbergen. The Mohns Ridge is characterized by oblique spreading under conditions of a thick cold lithosphere and narrow stable rift zone. The Gakkel and the Southwest Indian ridges are distinguished by the lowest spreading rate under the settings of the along-strike variations in heating of the mantle and of a variable spreading geometry. The intensity of endogenic structure-forming varies along the strike of the ridges. In addition to the prevalence of tectonic factors in the formation of the topography, magmatism and metamorphism locally play an important role.

DOI: 10.1134/S0016852113030023

INTRODUCTION

The rift zones of mid-ocean ridges (MORs) extend through out the oceans, making up a global system of about 70000 km length. The spreading rate, which varies from 0.7–1.3 to 16 cm/yr, is a key parameter that determines the topography and deep structure of spreading zones. In compliance with this parameter, MORs are subdivided into several types characterized by slow (<4 cm/yr), moderate (4–8 cm/yr), fast (8–12 cm/yr), and ultrafast (12–16 cm/yr) spreading rates. The Mid-Atlantic Ridge (MAR), Southeast Indian Ridge (SEIR), the northern and southern segments of the East Pacific Rise (EPR) represent the tectonotypes of these ridges, respectively. The accretion of the oceanic crust at spreading ridges is largely related to the generation and fractionation of primary melts of TOR-2 type according to the classification [7, 20], which are characteristic of all spreading zones of the World Ocean except for the North Atlantic. The primary magmas were generated by fractional polybaric melting of the oceanic mantle in the ascending column under a pressure of 20 to 8 kbar and at a temperature of $T = 1320\text{--}1250^\circ\text{C}$. The term TOR (Tholeiites of Oceanic Rifts) has been proposed by L.V. Dmitriev as a Russian equivalent to MORB. It was noted that the genetic types of TORs directly correlate with the parameter Na_8 [22], which indicates the primary Na content in the depleted tholeiitic melts [46]. Rift-related tholeiites variable in origin (TOR-1, TOR-2, Na-TOR and Si-TOR) are dis-

tinguished by different degrees of geochemical enrichment in lithophile elements and radiogenic isotopes, emphasizing the genetic and geochemical specificity of rift-related magmatism. N-, E-, and T-MORBs correspond to depleted, enriched, and transitional types of tholeiites. While general petrologic segmentation is mainly determined by geodynamic settings caused by global upwelling of mantle diapirs and regional tectonics, the geochemical features are controlled by a larger number of factors.

Studies performed in the 1990s–2000s showed that ridges with spreading rates less than 2 cm/yr and extending for ~20000 km differ from all other ridges, including those with a slow spreading rate [11, 15, 17, 19, 33, 50, 67], in the bottom topography, morphostructural segmentation, deep structure of the crust, magmatic activity, and crustal accretion mechanisms. These are a special type of ultraslow spreading ridges [8, 29, 36], which are mainly localized in the North Atlantic (Reykjanes, Kolbeinsey, Mohns, Knipovich, and Gakkel ridges) as a natural continuation of the MAR; they form a divergent boundary between the Eurasian and the North American lithospheric plates (Fig. 1). The Southwest Indian Ridge (SWIR), the American–Antarctic Ridge, and spreading ranges of the Red Sea and the Gulf of Aden are related to this type as well.

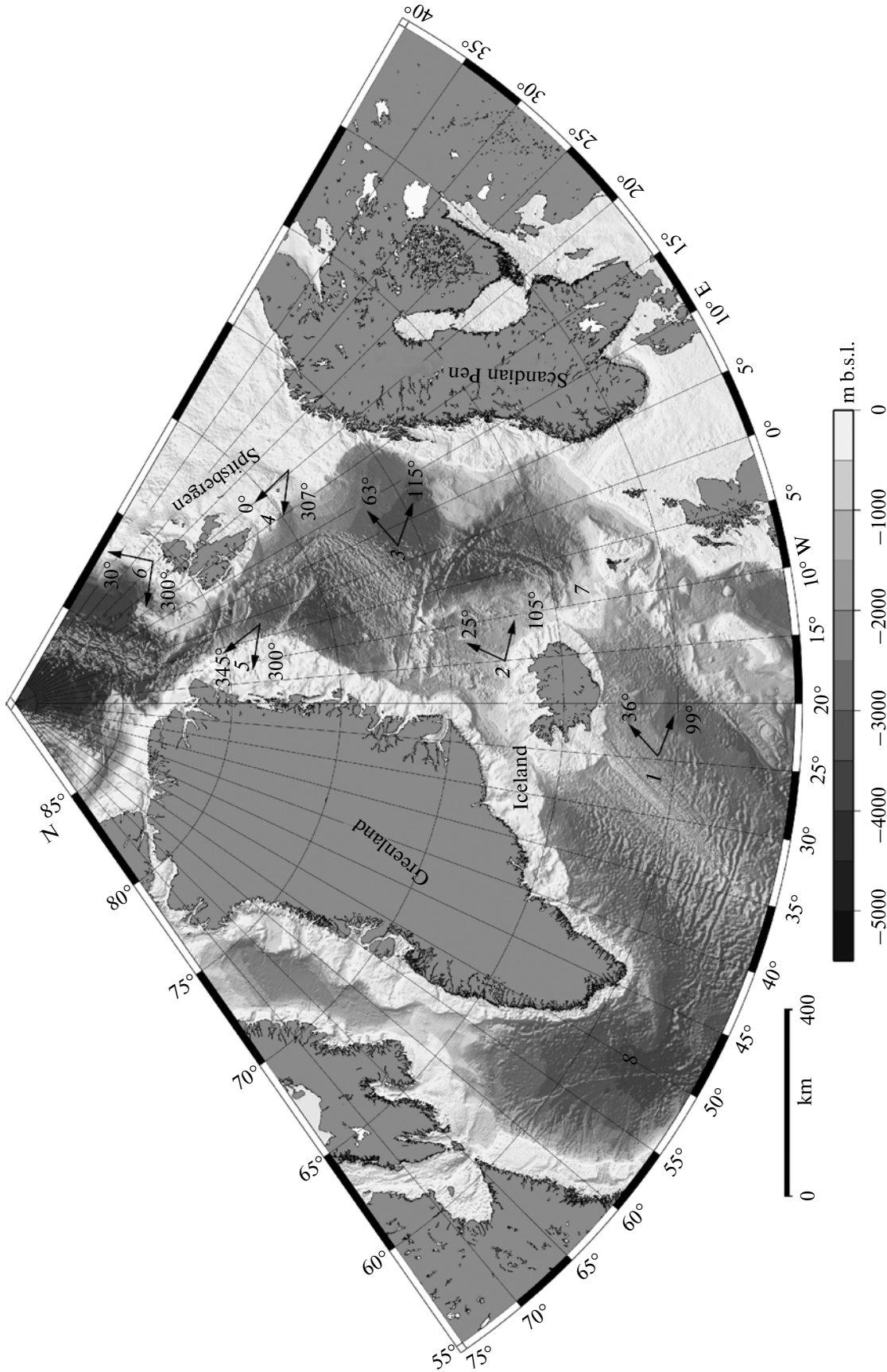


Fig. 1. Bathymetric map of Polar Ocean and North Atlantic to the north of the Bight TFZ, after [37]. Arrows indicate the directions of spreading and the strike of rift valley. Numerals in figure: 1, Reykjanes Ridge; 2, Kolbeinsy Ridge; 3, Mohns Ridge; 4, Knipovich Ridge; 5, Lena Trough; 6, Gakkel Ridge; 7, Aegir paleosspreading ridge; 8, paleosspreading center in the Labrador Sea.

This paper focuses on tectonic and magmatic features of rift zones of ultraslow ridges depending on geodynamic and kinematic settings of spreading.

STRUCTURE AND MAGMATISM OF SPREADING RIDGES IN THE NORTH ATLANTIC AND ARCTIC REGION

The Reykjanes Ridge is situated to the south of Iceland and extends for almost 900 km from the Bight Transform Fracture Zone (TFZ) to the Reykjanes Peninsula (Fig. 2a). The spreading rate varies from 18.5 mm/yr near Iceland to 20.2 mm/yr near the Bight TFZ [14, 35]. The ridge strikes at 036° NE and it is oblique to the spreading vector oriented of 099° ESE. Angle α between the direction of extension and the strike of the rift zone is 63°–65° (Fig. 2c).

Three morphological provinces characterized by the presence of a rift valley, of a transitional morphology, and by axial uplift give way to one another from south to north as approaching Iceland (Figs. 2c–2g). Seismic profiling of the ridge showed that the thickness of the crust in the eastern portion of the Reykjanes Peninsula is 21–22 km. In the Reykjanes Ridge, it is 13–14 km near 63° N [66], 9–10 km near 61° N, and 7.5–8.0 km near 58° N [61]. These values exceed the mean crust thickness (7.1 ± 0.7 km) in the slow-spreading MAR [67]. At a latitude of 58° N, the brittle layer reaches a depth of 16–17 km. Close to Iceland, near 61°30' N, its thickness is 9 km [59, 61]. Thus, approaching the Iceland thermal anomaly, the crust's thickness increases along the ridge, whereas the thickness of the brittle layer is reduced in the same direction; the heating zone becomes wider.

When the thickness of the brittle crustal layer is reduced, the rift zone topography and the faulting pattern change according to mechanisms characteristic for spreading ridges with transitional morphology [10]. Owing to predominantly oblique spreading, a system of en echelon arranged S-shaped fractures oriented nearly orthogonal to the direction of extension has been noted locally in the rift zone. The axial volcanic ridges are related to these fractures (Fig. 2b).

A crustal magma chamber was detected for the first time beneath the slow-spreading rift zone in the ridge segment between 57°36' and 57°51' N. The roof of this chamber is located at a depth of 2.5 km b.s.l. beneath the axial volcanic ridge with its center at 57°45' N. The magma chamber is filled with a crust–mantle mixture that contains no less than 20% of the melt with a melt lens near its roof [55, 61].

With increasing distance from the Iceland thermal anomaly, the character of the topography and morpho-structural segmentation gradually changes (Figs. 2b–2g). Variation in the morphology from axial uplift to rift valley is accompanied by progressively changing segment parameters. The length of axial volcanic segments diminishes from north to south, while the

dimensions of transverse nontransform offsets (TNOs) increase in the same direction (Fig. 2b) [18, 27, 52, 59].

The Kolbeinsey Ridge extends for 650 km to the north of Iceland from 67° to 71°40' N, i.e., from the Tjornes TFZ to the Jan Mayen TFZ. This rift system was formed as a result of jumping of the spreading axis, which had been initiated by the activity of the Iceland mantle plume in the Eocene and led to the abandonment of the Aegir Spreading Ridge [25, 51] (Fig. 1). The spreading rate at the contemporary Kolbeinsey Ridge varies from 18.5 mm/yr (67° N) at an azimuth of 105° ESE to 17 mm/yr (71°40' N) at an azimuth of 110° ESE [35]. Angle α between the extension axis and the rift zone strike is 80°–85°.

The Spar TFZ (69° N; offset, 34 km) and the Egvin TFZ (70°40' N; offset, 36 km) divide the Kolbeinsey Ridge into three segments [26]. The morphology of the southern segment is characterized by an axial uplift 40–50 km wide and 300–500 m high. The middle segment between the Spar and Egvin TFZs is characterized by transitional morphology with a reduced rift valley. Its width measures from 3 to 13–15 km; the depth varies from 500 m in the south to 1500 m in the north. The northern segment is characterized by a deeper and wider rift valley (up to 2.5 km wide and 15–20 km deep) [48]. Variation in axial morphology is effectively a result of changes of temperature and heat flow with increasing distance from Iceland [2].

In the segment 69°30'–70°20' N, the thickness of the crust beneath the ridge axis varies from 7.2 to 12 km [48]. It is 12.1 ± 0.4 km in the southern part and reduces to 9.4 ± 0.2 km to the north of 67°20' N [40]. As compared with the Reykjanes Ridge, the crustal thickness of the Kolbeinsey Ridge is 2–3 km less at the same distance from Iceland.

The asymmetric influence of the Iceland plume on the topography and structure-forming processes of the spreading Reykjanes and Kolbeinsey ridges is distinctly expressed in the rift zone morphology and along-axis dissection (Fig. 2h). Superfluous magma supply and heating of the mantle have been noted along the entire extent of the ridge; it is reflected in the increase in thickness of the crust.

The Mohns Ridge is a boundary between the Eurasian and North American plates between Jan Mayen Island and a point at 73°30' N and 8° E. Its length is about 580 km. The rift valley of this ridge strikes at 60° NE and the azimuth of spreading is 115° ESE [35]. Angle α is 55°. The spreading rate at the ridge is 16 mm/yr. This ridge is not offset by TFZs. The rift valley is located at a depth of 2500–3500 m, while the adjacent flank mountains are only 1000–2000 m deep. The rift valley deepens from 2200 to 3500 m from south to north.

The bottom topography of the rift zone is formed by a series of en-echelon axial volcanic ridges oriented at an azimuth of 30° NE [38]. Their length is 15–25 km and their elevation is 300–600 m above the bot-

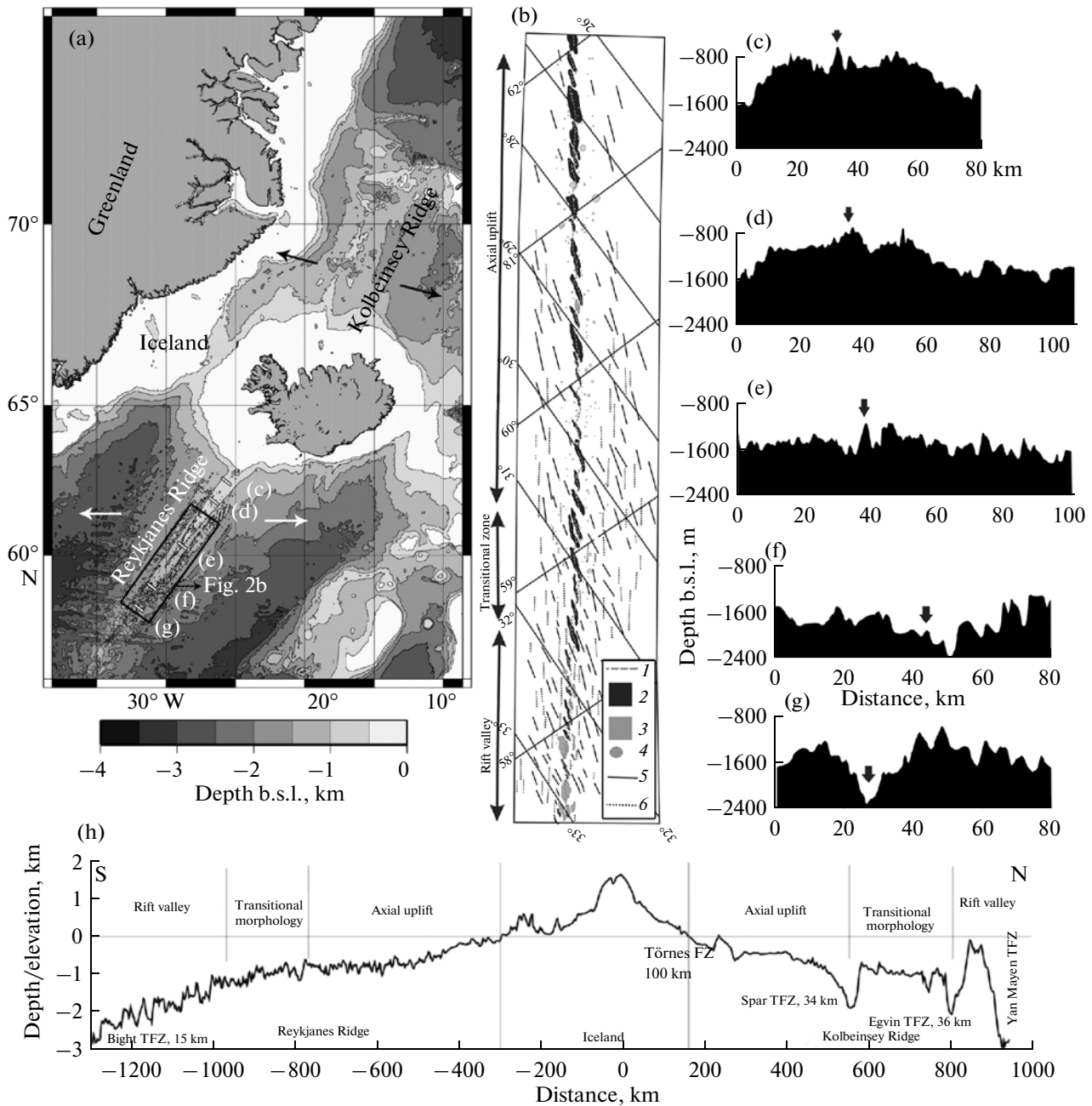


Fig. 2. Morphostructural features of the Reykjanes Ridge: (a) bathymetric map of region, after [37]; arrows indicate directions of spreading; (b) structural pattern of ridge segment from 57° to 62° N, modified after [44, 59]; (c) kinematic scheme; (d–g) bathymetric sections, after [44]; (h) topographic section along the rift zones of the Reykjanes Ridge, Iceland, and Kolbeinsey Ridge; distance is shown to the N and to the S from the center of the Iceland plume, modified after [40]. See Fig. 2a for location of section lines. (1) Spreading axis; (2) axial volcanic range; (3) basins related to transverse nontransform offsets; (4) volcanic center; (5) fault nearly parallel to axial volcanic range; (6) fault parallel to the rift zone of ridge.

tom of the rift valley. The volcanic ridges are separated by basins of amagmatic segments, which are 3.2 km deep, 20–25 km long, and devoid of any signs of magmatic activity. The basins are oriented nearly parallel to the direction of extension or the walls of the rift valley. The thickness of the oceanic crust beneath the ridge at 72°20' N and 1°30' E is 4.0–4.5 km, i.e., less

than the mean value for the crust of slow-spreading ridges [47], that most likely indicates less intense magma generation along the Mohns Ridge.

The Knipovich Ridge extends for more than 550 km along the continental margin of the Spitsbergen Archipelago from 73°45' to 78°35' N [33] as an element of a complex transitional zone between the

Mohns and Gakkel ridges (Fig. 1). The spreading rate in segments of orthogonal spreading is 15–17 mm/yr [35]. In segments of nonorthogonal divergence, the spreading rate decreases and the shear rate increases [34]. The ridge has a complex structure and a number of geological, geophysical, and geomorphic anomalies. This explains the diversity of interpretations of its tectonic evolution [11, 15, 16, 22, 25, 33]. In [33, 34, 54], the structure of the Knipovich Ridge is considered in terms of oceanic spreading and characterized as a young spreading center with ultraslow divergence. Other hypotheses interpret the ridge as a fault-line structure, a young oceanic rift, a TFZ with elements of pull-apart deformation, or a zone of disperse extension. The strike azimuth of the ridge changes near 75°50' N. To the north of this latitude, the ridge is oriented at 000°–007°(002° NE), while to the south, at 343°–350°(347° NW) [34]. The morphostructural and kinematic scheme of the Knipovich Ridge in Figs. 3a–3c is based on bathymetric and kinematic data [11, 33–35].

The key role in the morphology of the rift valley of this ridge is played by magmatic rises and amagmatic troughs. The rises with a relative elevation of more than 500 m above the bottom of the rift valley separate the valley into six segments (Figs. 3a, 3b). The segments vary in length from 30 to 145 km. The strike of these segments changes from 011° to 340° [33]. The elevation of rises above the rift valley bottom is 0.5–1.1 km. The rises are 4.5–18 km long and 3.6–13.7 km wide. All rises are oriented nearly orthogonal relative to the direction of extension. The magmatic rises separate troughs 3.4–3.7 km deep and 15–20 km wide at the edges and 9–14 km at the bottom [11, 16, 19, 33, 54]. The oceanic crust beneath the rift valley of the Knipovich Ridge is anomalously thin (3.0–3.5 km below troughs and 4.5–5.5 km below rises) [43].

The degree of deviation from orthogonal spreading progressively changes along the ridge. Angle α between the strike of the ridge's segments and the direction of divergence increases from 33° (segment B in the south with prevalence of shearing) to 63° (segment D in the north) [34].

Such kinematics of the ridge is supported by the mechanisms of earthquake sources that testify the substantial role and even prevalence of the shear component over the normal faulting [1]. An increasing shear component results in reduced magma generation, normal faulting, and as a consequence, modification of the ridge morphology. The degree of volcanic activity depends on angle α in each segment of the ridge [13].

Thus, the ridge is characterized by significant oblique shear component of spreading and, judging from the kinematics, occupies a transitional position between the TFZ and a typical spreading center. The magmatic rises are considered to be segments of focused volcanic activity, mantle upwelling, and normal faulting typical of the rift zones of MORs. Under the setting of significant shear component in the

spreading kinematics of the Knipovich Ridge, a system of troughs—nontransform offsets formed between the rises. Volcanism is strongly or completely reduced in these structural elements.

The Gakkel Ridge represents the northernmost segment of the boundary between the Eurasian and North American plates. The ridge strikes approximately for 1800 km from 6° W to 125° E. The spreading rate of the ridge varies from 14–15 mm/yr to 6–7 mm/yr, i.e., to the least value in the MOR system. Spreading is generally orthogonal in the ridge. The average strike of the ridge axis is 30°–50° NE, whereas the average orientation of the extension axis is 120°–140° SE [5, 35]. Angle α is 80°–100° except for the eastern segment, where the ridge bends to the north and spreading is complicated by a shear component with a decrease in angle α to 30°–40°. The Gakkel Ridge is not complicated by TFZs. The amplitude of nontransform offsets does not exceed 10–12 km.

The western volcanic, central amagmatic, and the eastern volcanic segments are distinguished in the ridge on the basis of morphological, geological, and geophysical features (Figs. 4a–4c) [31, 32, 50]. The western volcanic segment extends for 220 km from 7° W to 3° E (Figs. 4b, 4c). The spreading rate varies here from 15 to 13.5 mm/yr. The bottom of the rift valley is located at a depth of 3.8–4.0 km. Large volcanic rises 1.2–1.5 km high are spaced at 20–30 km. The length of the volcanic rises is 15–50 km; the width of bottom in the rift valley bounded by rift terraces is 10–18 km (Fig. 4e). The crustal thickness is 2.5–4.9 km [42]. Mainly basalts have been dredged [50]. The number of volcanoes in the rift zone reaches 55% of their total number in the MAR segment from 22° to 26° N. Their density is 31 items per 1000 km² and their average elevation is 29.5 m above the bottom of the rift valley, that is, two times less than in the MAR [31].

The central amagmatic segment from 3° to 30° E extends at about 300 km (Figs. 4b, 4c). The spreading rate varies from 13.5 to 12.7 mm/yr. At a spreading rate less than 13.5 mm/yr estimated to the east of 3° E, where the rift axis abruptly deepens by 1.5 km (Fig. 4c). Only one large volcanic center at 19° E has been noted over the entire extent of this segment. No fresh lava flows or volcanic edifices were revealed in the rest of the rift valley [31, 32]. The volcanic edifices are localized only at the shoulders of the rift valley. The lack of magmatic activity is combined with a nearly orthogonal extension. The bottom of the rift valley is located at a depth of 5000–5500 m and consists of a series of elongated basins (Fig. 4a). At the transverse section, the V-shaped rift valley is bounded by low-angle (20°–25°) slopes, which are not disturbed by normal faults. The off-axis topography is characterized by swell-shaped uplifts 1.5–2.0 km high with low-angle symmetric slopes and narrow (1–2 km) crests (Figs. 4d, 12c) without indications of normal faulting or volcanic activity. The width of such uplifts reaches 12–20 km.

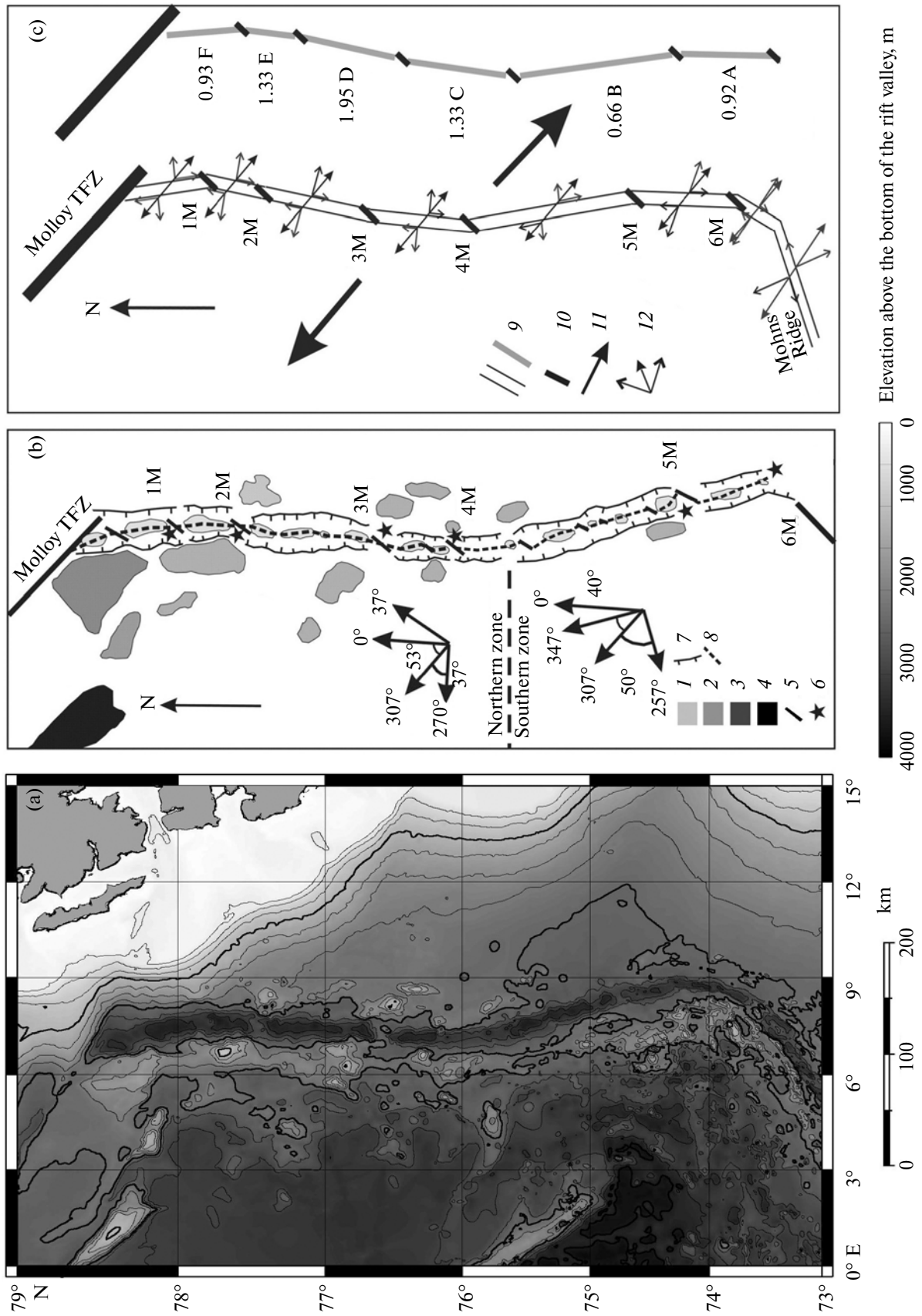


Fig. 3. Morphostructural and kinematic features of Knipovich Ridge: (a) bathymetric map of ridge and adjacent region, after [37]; (b) morphostructural scheme; arrows indicate kinematic parameters of spreading, after [34]; (c) kinematic scheme. (1) Basin; (2) off-axis trails of magmatic uplifts; (3) uplift of interior angle of the Molloy TFZ; (4) Hovgaard microcontinent; (5) axis of magmatic uplift; (6) the largest magmatic uplift with relative elevation more than 500 m above the bottom of the rift valley; (7) edge of rift valley; (8) spreading axis; (9) amagmatic segment; (10) magmatic segment; (11) direction of regional plate divergence; (12) kinematic components of spreading (spreading vector is depicted by the middle arrow between the shear and the extensional components). Symbols in figure: 1M–6M, magmatic segments; A–F, amagmatic segments. Numerals near symbols A–E denote ratios between shear and tensile stresses in spreading kinematics of each segment.

Identical structures were described by Cannat et al. [29] in the off-axis part of the amagmatic segment of the ultraslow SWIR. The crustal thickness in the central amagmatic segment of the Gakkel Ridge is only 1.3–2.5 km and does not exceed 2 km, on average [42]. Gabbro and peridotite dominate in the rift valley [50].

The extent of the eastern volcanic segment is ~600 km from 30° to 94° E (Figs. 4b, 4c). The spreading rate varies here from 10 to 12.7 mm/yr. The main feature of local topography is characterized by the occurrence of large uplifts oriented orthogonal to the rift axis. The distance between them varies from 50 to 150 km (Fig. 4b). At the bottom of the rift valley, volcanic rises up to 1.5–2.0 km high and 20–35 km long correspond to these uplifts. The bottom of the valley is located at a depth of 4.5–5.0 km and its width is 12–15 km. The steep slopes of the valley are dismembered by normal faults. The crustal thickness increases locally near the volcanic edifices. The thickness of the crust in the adjacent basins is limited to 2.5–3.3 km [41, 42]. Uplifts resembling accretionary swells characteristic of the central segment do not occur in the rift mountains or on the flanks of the ridge. The off-axis topography is distinguished by plateau-like elevations with tops at a depth of 3.5–4.0 km. The density of volcanic edifices is 14.4/1000 km²; their average elevation is 22.9 m [31].

Thus, the Gakkel ridge exhibits three different geodynamic settings of ultraslow spreading. In the western volcanic segment, the style of accretion, topography, and geological structure is close to that of the slow-spreading ridges; however, the volcanic activity and crustal thickness are lower than at the MAR. The dry spreading is typical of the central segment. The crustal thickness is thinnest here, and the mantle rocks are exposed at the seafloor. This is probably caused not only by spreading slower than 13.5 mm/yr and low-intensity magma supply, but also by relatively low temperature of the mantle. In the eastern segment, the volcanic activity is somewhat higher but remains lower than in the western segment.

The magmatic activity of the ridges in the North Atlantic and the Arctic Region reveals specific genetic and geochemical features typical for the Reykjanes and Kolbeinsey spreading ranges (Fig. 5), which are characterized by tholeiitic eruptions from a significant depth (TOR-1 type). The primary magmas are formed

in the course of polybaric fractional melting of the oceanic mantle within the ascending mantle column at a released pressure varying from 25 to 10 kbar and at a temperature of 1350–1300°C (Fig. 5).

Basalts of the Reykjanes Ridge were formed in the course of fractionation of deep-seated TOR-1 melts. They crystallized in shallow-seated transitional magma chambers under a pressure of 1–2 kbar with advanced differentiation up to 65–70% (MgO ranges from 13.5 to 5.0 wt %). Iceland, which is situated in the spreading region, exerted a substantial effect on the thermal regime of the lithosphere and the growth of the Reykjanes Ridge, facilitating development of shallow-seated chambers beneath the range. The TOR-1 melts crystallized mostly under dry conditions (Fig. 5a). TOR-1 melts relatively enriched in potassium and other lithophile elements occur near Iceland and do not appear north of 52° N. Volcanic glasses at the Kolbeinsey Ridge are comparable with the TOR-1 type and classified as derivatives of the primary TOR-2 melt near the Jan Mayen TFZ.

The volcanic glasses from the Knipovich and Gakkel ridges are characterized by the elevated sodium contents. Two levels of Na concentrations related to the TOR-2 type and comparable with evolved Na-type tholeiites are distinguished. In addition to the elevated Na contents, the glasses are enriched in Si and depleted in Fe. This type of melts is also known from the Cayman Trough, at the Antarctic–Australian discordance [46], and in the Equatorial Atlantic. It is especially typical of the Gakkel Ridge with a colder lithosphere [64]. Connection between petrochemical types of basalts and depth of rift zones is clearly observed (Fig. 5a). The Na-TOR tholeiites are localized in deeper segments of the rift zone.

The geochemical heterogeneity determined by the participation of the depleted and the enriched sources in the melting beneath the present-day rift zones of the North and Polar Atlantic (Fig. 5a–5d) opens up possibilities for geochemical segmentation of magmatism therein. While the appearance of anomalous tholeiites enriched in lithophile elements and radiogenic isotopes in the Reykjanes and Kolbeinsey ridges is directly related to the development of the Iceland plume, the anomalies of the Mohs (southern end), Knipovich, and Gakkel ridges (Figs. 5b–5d) have other sources. The most intense anomaly in the polar

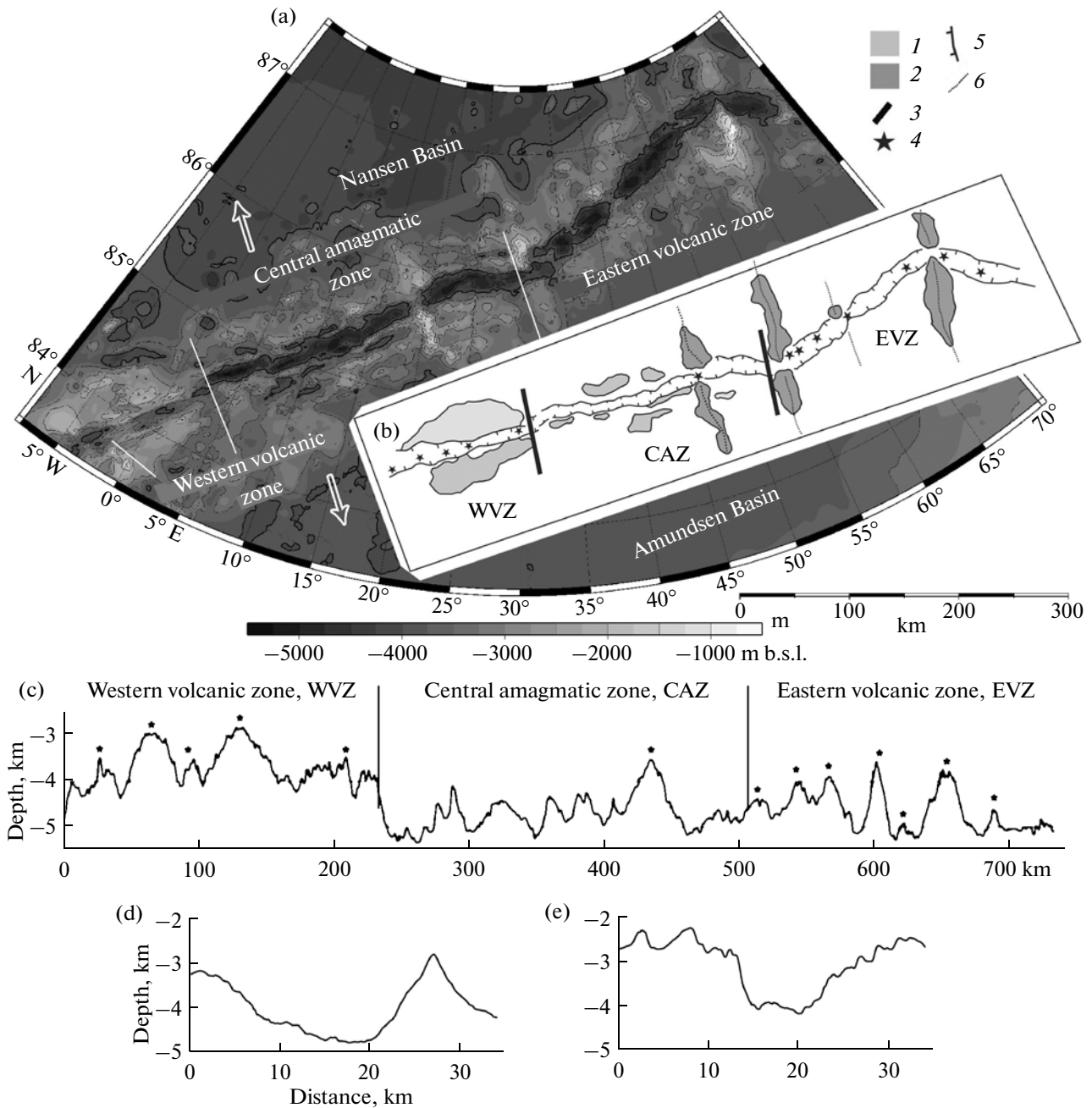


Fig. 4. Morphostructural features of Gakkel Ridge: (a) bathymetric map of the ridge and adjacent region, after [37]; (b) structural scheme of the ridge; (c) along-axis bathymetric profile, after [50]; (d, e) transverse bathymetric profile, after [32]. (1) Uplifts of rift mountains; (2) axis-perpendicular rises; (3) boundaries of geomorphic provinces of the ridge; (4) volcanic center; (5) edge of rift valley; (6) axes of axis-perpendicular rises.

region is confined to the Lena Trough. In the Knipovich Ridge, this anomaly increases northward approaching the Lena Trough [53]. The Gakkel Ridge is distinctly divided into two provinces. The western province is distinguished by the depleted Na-TOR tholeiites (Fig. 5d). The enriched tholeiites with ele-

vated concentrations of radiogenic Pb, Sr and lower $^{143}\text{Nd}/^{144}\text{Nd}$, which are the most abundant in the Gakkel Ridge, are also noted in the Knipovich and Mohns ridges, as well as in the plateau-basalt complexes and alkaline lavas of Spitsbergen. At the same time, enriched tholeiites with $^{87}\text{Sr}/^{86}\text{Sr}$ up to 0.704,

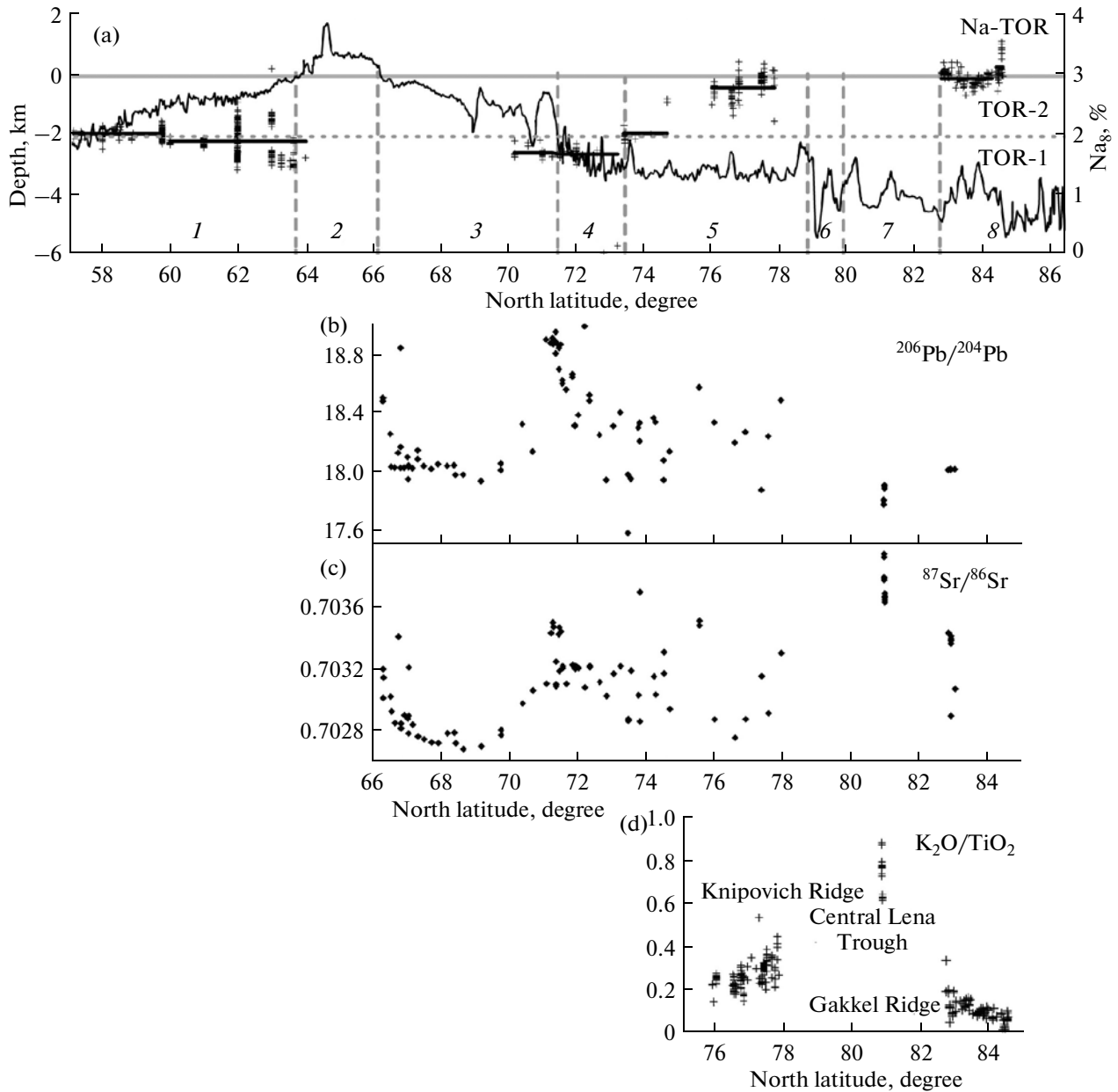


Fig. 5. Variations in composition of glasses from spreading ridges of North Atlantic and Arctic region, after [22, 53, 64]: (a) along-axis section of depths and variations in the Na concentrations corresponding to 8 wt % MgO, which reflect the Na concentrations in primary melts generated in the mantle beneath ridges, after [46]; the Na₈ parameter correlates with compositions of TOR-1, TOR-2, and Na-TOR types of primary tholeiitic melts [22] derived from lherzolitic mantle at various depths; (b, c) variations in ²⁰⁶Pb/²⁰⁴Pb and ⁸⁷Sr/⁸⁶Sr isotope ratios in glasses from ridges of North Atlantic; geochemical anomalies near Iceland, Jan Mayen Island, and Lena Trough are noted; in general, magmatism of Knipovich and the Gakkel ridges have enriched geochemical characteristics; (d) degree of geochemical enrichment of tholeiitic melts in Polar Atlantic expressed in K₂O/TiO₂ ratio. The highest anomaly is related to central segments of the Lena Trough. Two provinces are distinguished in Gakkel Ridge. More enriched tholeiites are localized in the eastern province. Profile (a): (1) Reykjanes Ridge; (2) Iceland I.; (3) Kolbeinsey Ridge; (4) Knipovich Ridge; (5) Sptsbergen Shear Zone; (6) Lena Trough; (7) Gakkel Ridge.

low ²⁰⁶Pb/²⁰⁴Pb (17.6) and ¹⁴³Nd/¹⁴⁴Nd (0.5128), and elevated concentrations of radiogenic Pb are found in the central Lena Trough. This is explained by involvement of the ancient phlogopite- or amphibole-bearing subcontinental lithospheric mantle in melting [53].

Thus, the North and Polar Atlantic ridges clearly demonstrate the influence of the Iceland plume on magmatism expressed in the depth of magma generation (TOR-1 type) and fractionation of primary magma in transitional chambers. At the same time, the

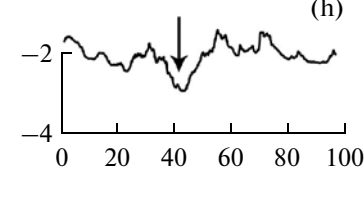
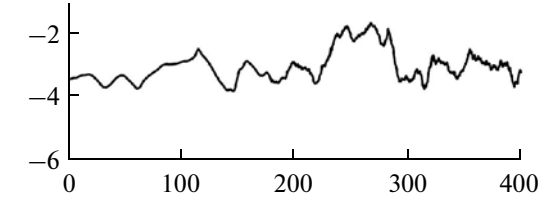
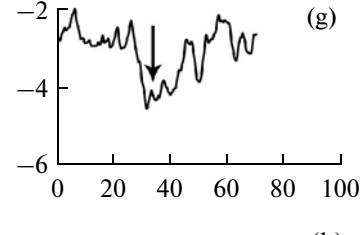
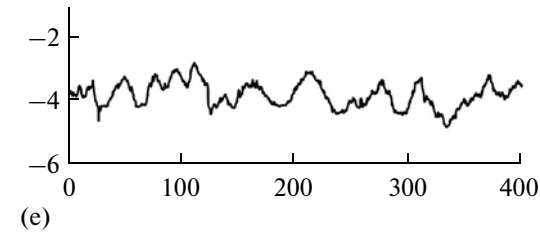
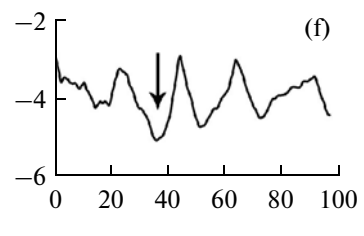
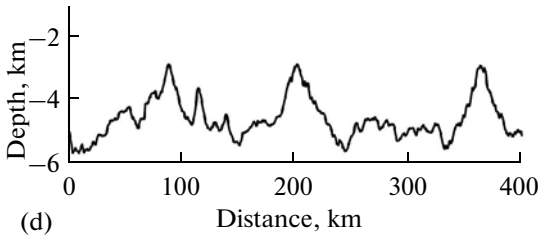
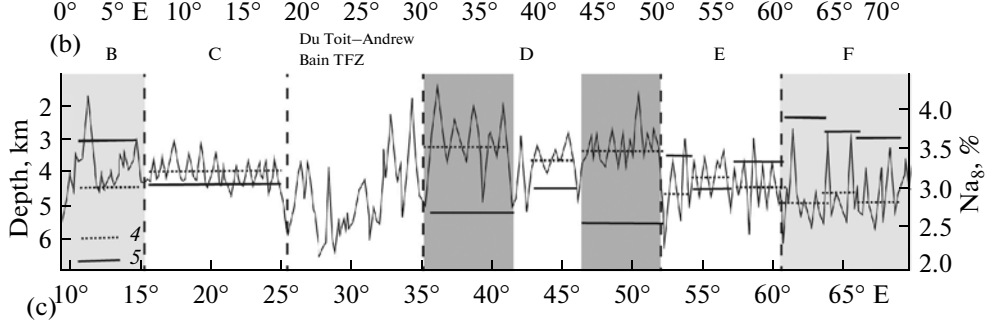
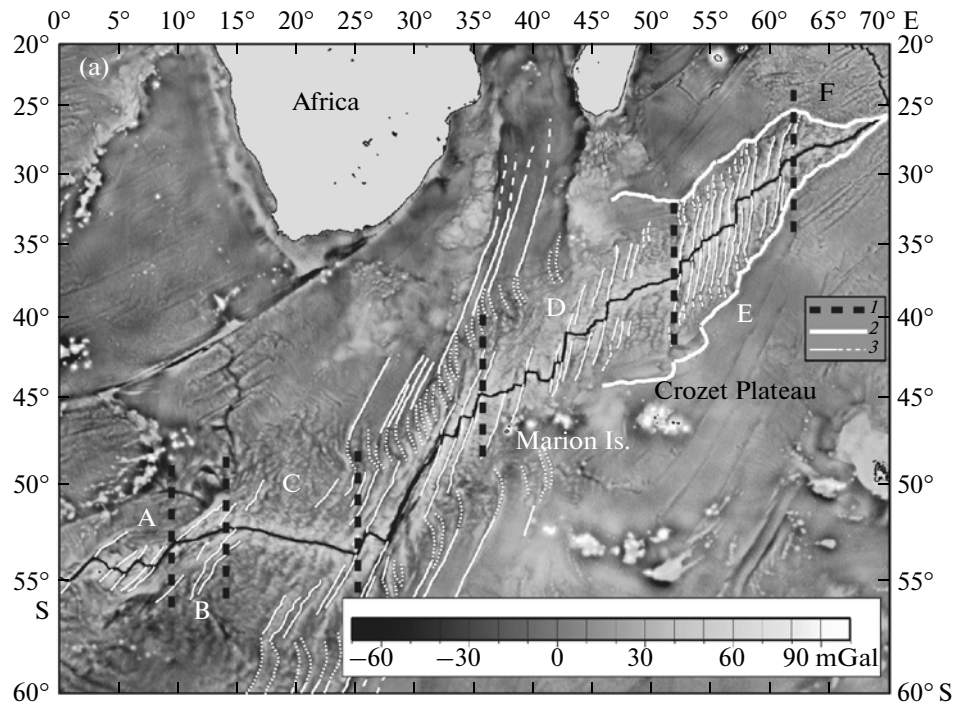


Fig. 6. Structure of SWIR: (a) tectonomagmatic provinces A–E and structural elements of adjacent region against the background of the gravity anomaly map, after [56, 58]; (b) along-axis section of bottom topography of ridge, after [30]; segments with elevated and lower temperatures of mantle are shown by dark and light gray, respectively; (c, f) along-axis and across-strike bathymetric profiles of province F, respectively; (d, g) along-axis and across-strike bathymetric profiles of province C, respectively; (e, h) along-axis and across-strike bathymetric profiles of province D, respectively; arrows indicate spreading axis. (1) Boundaries of provinces; (2) off-axis trails of TFZs; (3) suture zone between the SWIR and the SEIR lithosphere; (4) average depth in province; (5) average Na₂O content in basalt of province, after [30].

Knipovich and Gakkel ridges, which are forming by colder lithosphere, demonstrate the shallower magma generation (Na-TOR) and geochemical anomalies related to the involvement of fragments of the continental lithospheric mantle in melting.

STRUCTURE AND MAGMATISM OF THE SOUTHWEST INDIAN RIDGE

The SWIR extends for 7700 km in the SW–NE direction from the Bouvet triple junction (55° S, 0°40' E) to the Rodriguez triple junction (25° S, 70° E) (Figs. 6a, 6b) [58]. The obliquity of spreading at the ridge widely varies: the angle α changes from 32° to 90°. The effective spreading rate increases from 8 to 16 mm/yr with growing obliquity of the spreading axis. Wide variations in basalt and peridotite compositions are noted as well (Fig. 6b) [60]. The Bouvet hotspot in the western segment of the ridge, the Marion hotspot in its central segment, and the Crozet hotspot in the eastern segment (Fig. 6a) indicate that thermal regime is heterogeneous along the ridge [57].

The ridge is subdivided into two parts by the giant demarcation system of the Prince Edward–Andrew Bain TFZ, which offsets the spreading axis for 1100 km (Fig. 6a). This TFZ is out of the scope of this paper. The eastern SW–NE-trending part of the ridge is segmented by frequent TFZs, whereas its western near-latitudinal part (the African–Antarctic Ridge) is almost devoid of TFZs. The geomorphic and geological–geophysical features of the ridge, along with the kinematics and geometry of spreading, allow us to outline a number of provinces (Fig. 6) characterized by specific topography of the rift zone, morphostructural segmentation, and intensity of tectonic, magmatic, and metamorphic processes reflected in the topography (table).

Province A is a segment that extends 400 km from the Bouvet triple junction to the Shaka TFZ and is characterized by a reduced rift valley 1.5–2.0 km deep with large volcanic rises in its axial zone. At local sites, the volcanic edifices tower above the valley edges by 200–300 m. The depth of the bottom of the valley is 1.5–3.0 km. Spreading is orthogonal. The topography forms due to the influence of the Bouvet hotspot. Similar features of the topography are typical of the ridge segment in **province D**, which extends between the Prince Edward and Gallieni TFZs (Figs. 6e, 6h). In the Bouvet triple junction, the spreading axis is localized in the axial uplift of the Spiess Ridge up to 2 km high and with a minimum depth of 1.0–1.5 km.

The segment of the ridge within **province B** extends for 400 km from the Shaka TFZ to the nontransform discontinuity at 16° E. This province is characterized by a combination of extended amagmatic and short magmatic segments (Fig. 6c). Segmentation is formed under the setting of strongly oblique spreading ($\alpha = 36^\circ\text{--}58^\circ$) and a low effective spreading rate (8.7–13.9 mm/yr). A similar structure is noted for **province F**, which extends from the Melville TFZ to the Rodriguez triple junction. These provinces are characterized by a combination of extended amagmatic segments with a maximum depth of the rift valley (4.5–5.7 km) and short magmatic segments with minimum depth (2.5–3.0 km) (Figs. 6b, 6c) [29, 30, 36]. The segmentation is formed under the setting of strongly oblique spreading ($\alpha = 36^\circ\text{--}58^\circ$) and an extremely low effective spreading rate (8.7–13.9 mm/yr). The amagmatic segments are characterized by swell-shaped uplifts on the ridge's flanks, prevalence of serpentinized peridotites in dredges, and thin crust (0–3.5 km) (Fig. 6f). The structure of the ridge within provinces A and E is similar to that of the central amagmatic segment in the Gakkel Ridge.

Province C extends for 750 km from the nontransform discontinuity at 16° E to the Du Toit TFZ (25° E). The axial volcanic rises separated by low-amplitude (up to 10–15 km) nontransform offsets localized at the bottom of the valley (Fig. 6d). Spreading in this province is nearly orthogonal ($\alpha = 70^\circ\text{--}85^\circ$, and effective spreading rate is 15.6–16.0 mm/yr). The morphometric parameters of the bottom topography are close to the values characteristic of the MAR. As in the MAR, the off-axis topography is formed by asymmetric blocky uplifts. The western magmatic segment of the Gakkel Ridge has a similar structure.

In **province E**, the ridge's segment extends for 1100 km from the Gallieni TFZ to the Melville TFZ. Small TFZs with offsets of up to 55–70 km, large TFZs with offsets more than 100 km, and short orthogonal and extended oblique segments (reduced amagmatic and distinctly expressed magmatic) are juxtaposed here. Spreading developed as a result of eastward migration of the Rodriguez triple junction and frequent changes in the kinematics. Spreading is slightly oblique or nearly orthogonal ($\alpha = 60^\circ\text{--}85^\circ$; the effective spreading rate is 11.9–14.0 mm/yr).

In general, various geodynamic settings of ultraslow spreading, which were noted above for the spreading ridges of the North Atlantic and Arctic Region, are recognized along the strike of the SWIR. They are reflected in geomorphic and geological–geophysical features, as well as a deep structure of the ridge.

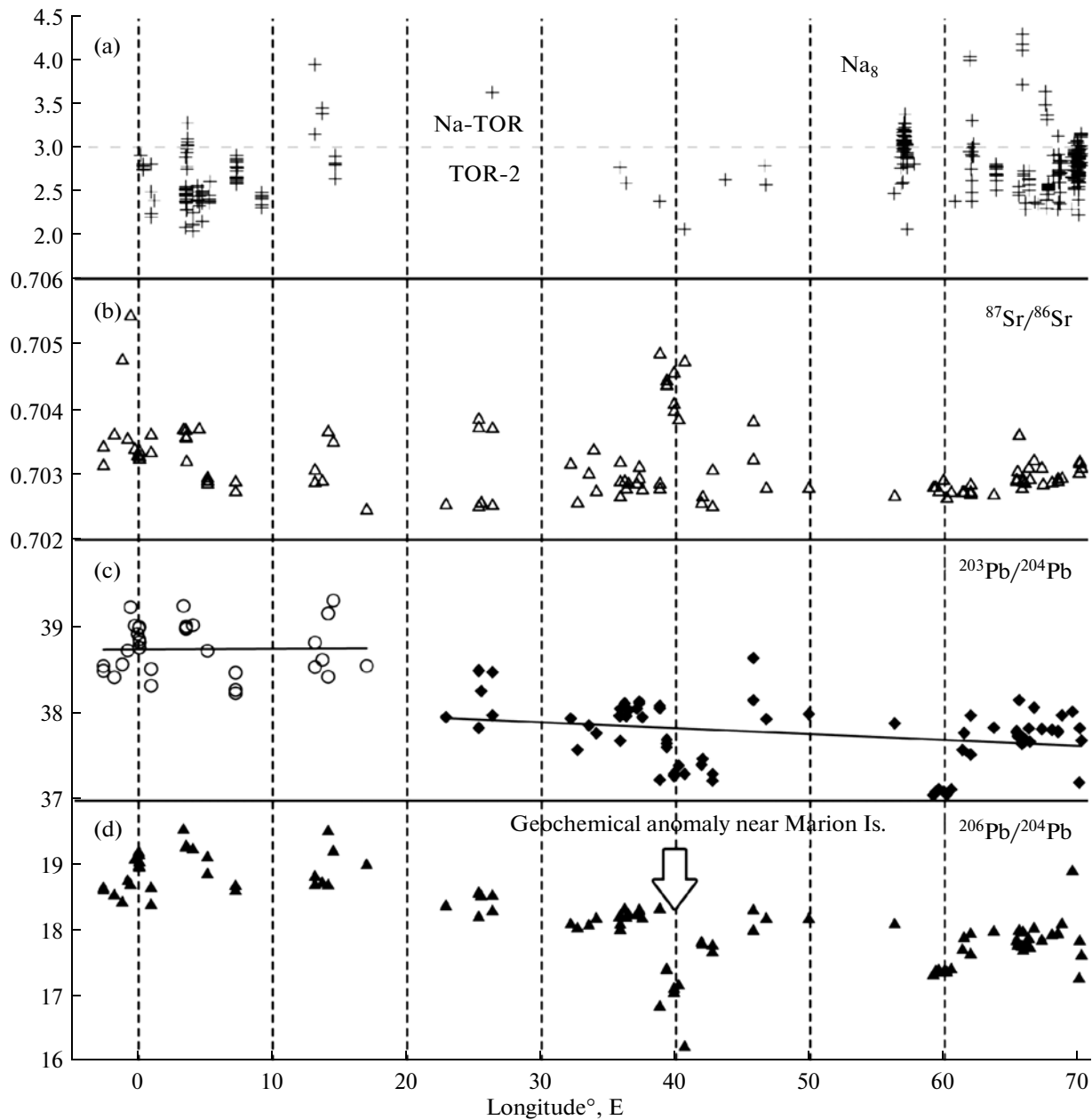


Fig. 7. Variations in Na_8 and isotopic parameters of glasses of the SWIR from the Bouvet to the Rodrigues triple points, after [21, 22 and references therein]. As is seen from panel (a), TOR-2 tholeiites dominate in the ridge. Eruptions of Na-TOR tholeiites related to a shallow-seated magma source are noted only at 14–15° E near the Rodrigues triple point. According to the isotopic data (panels b–d), two large geochemical provinces are distinguished. The western province is enriched in radiogenic elements, and the eastern province coincides with the tectonic segments separated by the Prince Edward–Andrew Bain TFZ. An isotopic anomaly near Marion Island corresponds to the tholeiites with a low $^{206}\text{Pb}/^{204}\text{Pb}$ and an elevated $^{87}\text{Sr}/^{86}\text{Sr}$ values that is interpreted as the DUPAL anomaly related to participation of the older lithosphere in melting.

The tholeiites derived from TOR-2 and distinguished by a Na_8 level close to 2.8–3.0 dominate in the tectonic segments of the SWIR. Variations in Na_2O contents in glasses from the SWIR corresponding to 8 wt % MgO [46] (Fig. 7; table) reflect the initial concentrations in primary melts. As is seen from Fig. 7, melts developed near the Bouvet triple junction (TOR-1 type with lower Na_8 and Si_8 in combination

with higher Fe_8) occupy a special position, emphasizing the effect of the Bouvet hotspot on magmatism of the SWIR similar to the influence of the Iceland plume on the Reykjanes and Kolbeinsey ridges.

In **province B** (10°–16° E), tholeiites of the Na-TOR type with higher Na_8 values (>3) generated at a shallower depth erupted along with tholeiites of the TOR-2 type. Na-TOR-type tholeiites also occur in

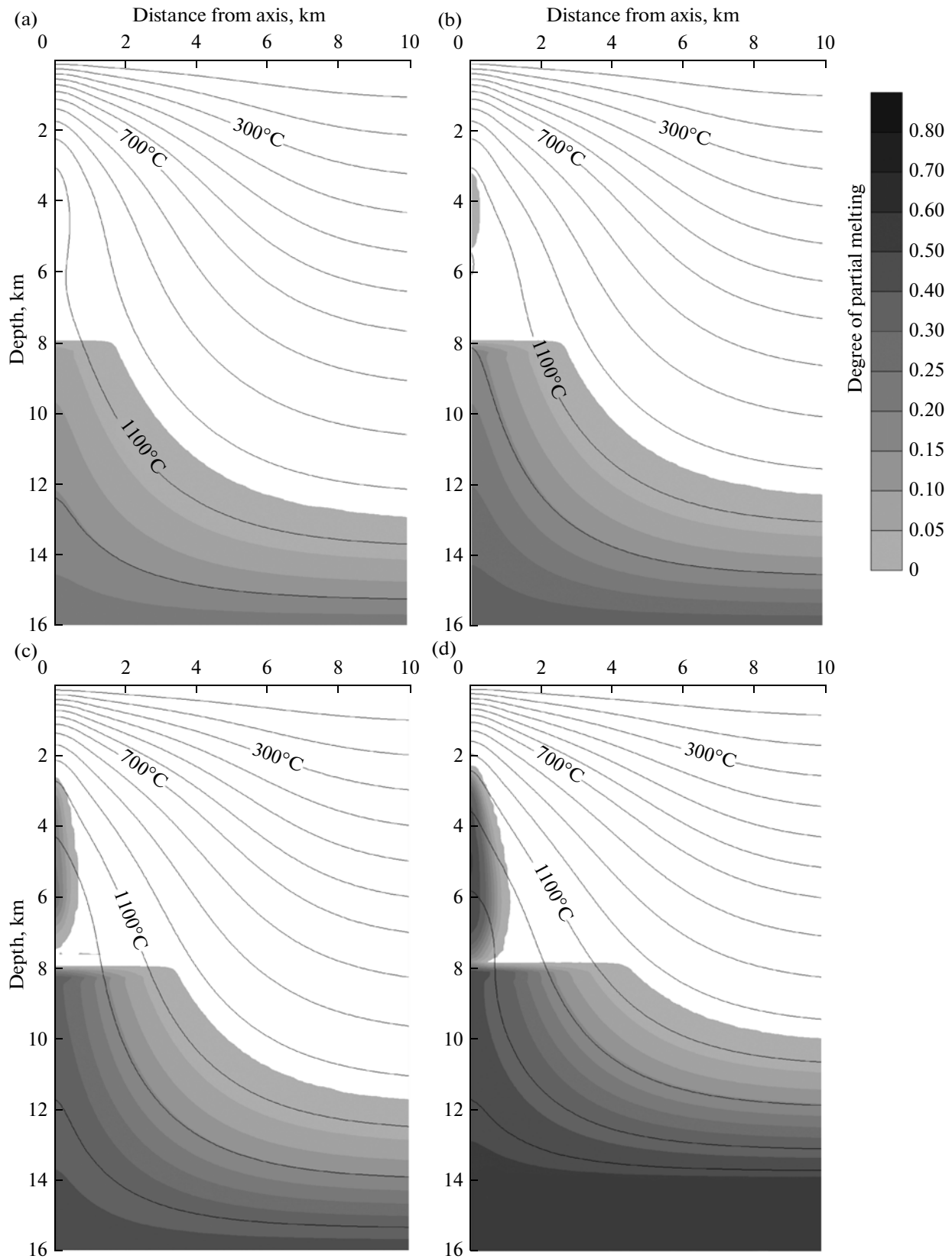


Fig. 8. Temperature and degree of partial melting in axial spreading zone at spreading rate of 2 cm/yr and thickness of crust of 8 km versus heating of mantle, °C: (a) 1250, (b) 1300, (c) 1350, (d) 1380. Isotherms are spaced at 100°C.

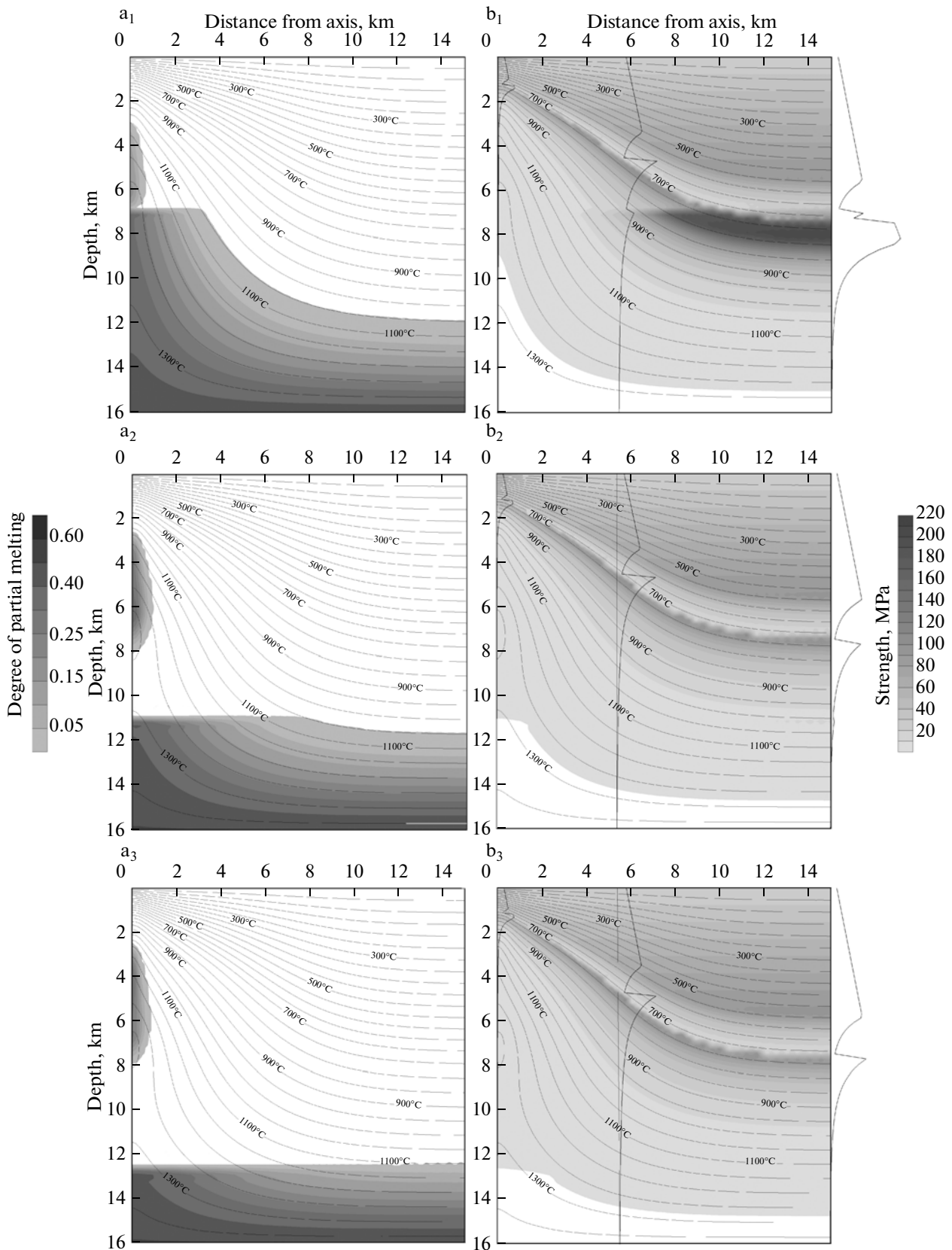


Fig. 9. Temperature and degree of partial melting in axial zone of ultraslow spreading ridge at spreading rate of 2 cm/yr and mantle temperature $T \geq 1350^\circ\text{C}$ depending on thickness of crust, km: (a₁) 7, (a₂) 11, (a₃) 12.7 and strength of rocks in oceanic lithosphere calculated using the thermal model. Curves of variation in strength with depth for distances from ridge axis, km: (b₁) 0, (b₂) 5.5, (b₃) 15.5.

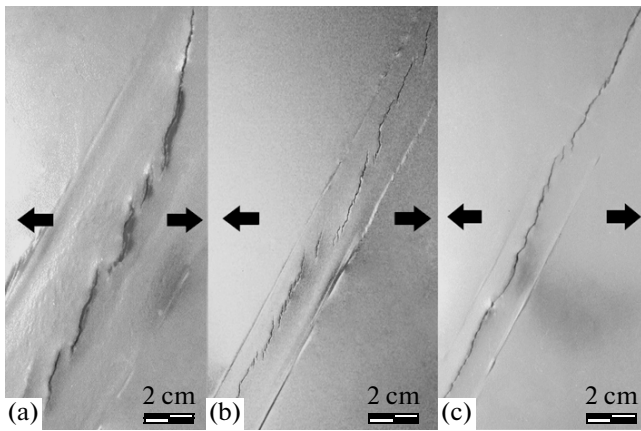


Fig. 10. Experimental results on simulation of the formation of the axial zone structure in the Reykjanes Ridge: photographs, view from above. Runs reproducing settings in (a) northern province: $H = 1$ mm, $W = 5$ cm; (b) central transitional province: $H = 2$ mm, $W = 2$ cm; (c) southern province: $H = 3$ mm, $W = 2$ cm.

province F near the Rodriguez triple junction. They are characteristic of the coldest provinces of slow-spreading zones such as Gakkel and Knipovich ridges in the Polar Atlantic.

The central part of the SWIR (Fig. 6, provinces B–E) is characterized by the occurrence of basalts derived from TOR-2, but the type of tholeiitic magmatism found near 40° E is not known in any other spreading ridges of the World Ocean. These are Si-type melts with high Si_8 and Fe_8 concentrations combined with low Na_8 values (Fig. 7). Glasses of this type were found in only one dredge near 39° E and close to the Rodriguez triple point. In the latter locality, they have no clearly expressed attributes. Their Ti and Na contents are somewhat higher, whereas the Fe contents are lower than in other glasses, probably owing to mixing with normal TOR-2 and Na-TOR tholeiites [21, 23]. Si-type melts are distinguished by enrichment in silica together with low Ti and Na contents. Sources of Si-type and TOR-2 melts identified near the 39° – 40° E

are characterized by the incorporation of matter pertaining to the EM-1 mantle reservoir (extreme DUPAL anomaly) with low $^{206}Pb/^{204}Pb$ (below 17.0) and high $^{207}Pb/^{204}Pb$, $^{208}Pb/^{204}Pb$, and $^{87}Sr/^{86}Sr$ ratios (Figs. 7b–7d). The composition of this source probably indicates an admixture of the continental lithospheric material of the ancient Gondwana landmass. An enriched mantle source of tholeiites in the western SWIR near the Bouvet triple point is also similar in composition to the HIMU component with high Pb isotope ratios and a lower $^{143}Nd/^{144}Nd$ ratio at a moderate $^{87}Sr/^{86}Sr$ value, but these isotope ratios do not reach the HIMU level, indicating a hybrid origin of the source (HIMU + EM-2) (Figs. 7b–7d). Thus, in general case, two large geochemical provinces—western and eastern—are distinguished. They coincide with the tectonic megasegments related to the evolution of the oceanic crust specific to each domain. It should also be emphasized that tholeiites enriched in Na_2O and depleted in FeO and derived from shallower sources occur in the SWIR as in the colder domains of the ascending mantle in the Gakkel and Knipovich ridges. In the SWIR, they are localized in the western segment (province B, 12° E) and close to the TFZ (province F) in the young region at the eastern end of the SWIR.

TOR-1 tholeiites related to deeper sources occur near the Bouvet hotspot, and this situation is similar to the localization of such melts of the Reykjanes and Kolbeinsey ridges near Iceland (Fig. 5a). As the northern segment of the Reykjanes Ridge, the Spiess Ridge at the western end of the SWIR reveals favorable conditions for fractionation of primary magmas in transitional chambers.

CONDITIONS OF FORMATION OF MAGMA CHAMBERS UNDER CONDITIONS OF ULTRASLOW SPREADING

A nonstationary numerical model for the formation of crustal magma sources based on the principles of discrete–continuous spreading assumes formation

Large provinces in Southwest Indian Ridge

Province	Province boundaries	L , km	H_{aver} , m	D , °	R , °	α , °	$90-\alpha$, °	$SR/2$, mm/yr	$SR_{eff}/2$, mm/yr	MBA, mGal	$Na_{8,0}$, %
A (3° – 9° E)	Bouvet TP–Shaka TFZ	400	3220	42	125	83	7	7.8	7.75	–80	2.70
B (9° – 16° E)	Shaka TFZ– 16° E TNO	360	3971	37	84	48	42	8.13	5.78	–59	3.55
C (16° – 25° E)	16° E TNO–Du Toit TFZ	640	3961	35	112	77	13	7.95	7.79	–54	3.23
D (35° – 52° E)	Prince Edward TFZ–Gallieni TFZ	1010	3451	5	75	70	20	7.38	6.95	–90	2.80
E (52° – 60° E)	Gallieni TFZ–Melville TFZ	1020	4344	2	70	68	22	7.03	6.43	–26	3.27
F (60° – 70° E)	Melville TFZ–Rodriguez TP	1040	4696	0	62	62	28	6.65	5.91	–15	3.76

Notes: Data on kinematics of spreading are given after [30, 35]; Na_8 and mantle Bouguer anomaly (MBA), after [30]; bathymetric data, after [29, 36, 37, 39, 57, 58]. SR , spreading rate; TP, triple point; TFZ, transform fracture zone; TNO, transverse nontransform offset. See text for other symbols.

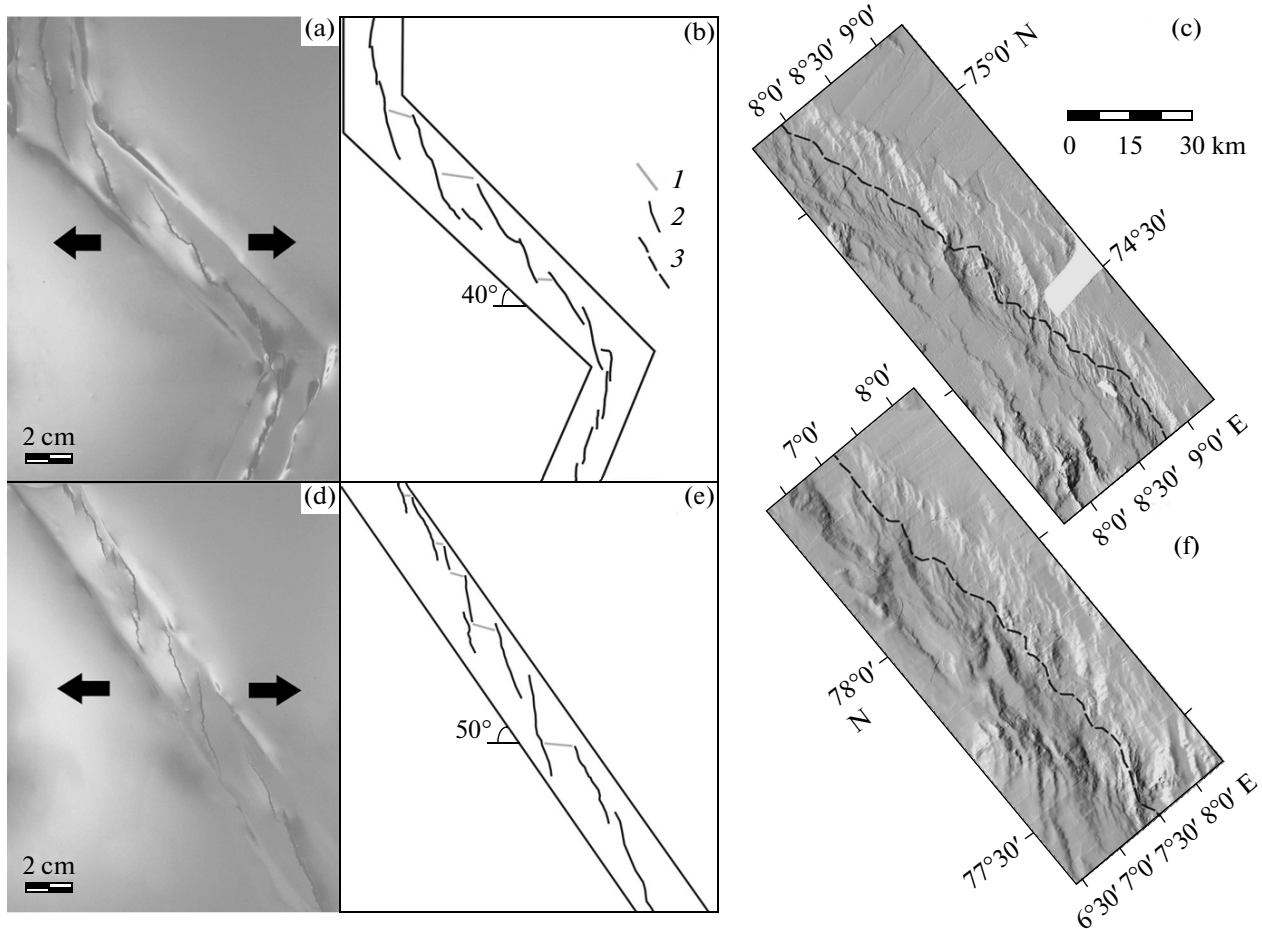


Fig. 11. Experimental results of an oblique extension in weakened zone of the Knipovich Ridge model; (a–c) $\angle\alpha = 40^\circ$, (d–f) $\angle\alpha = 50^\circ$; (a, d) photographs of runs and (b, e) their interpretation; (c, f) bathymetric maps of southern segment with pull-apart basin in its central part and northern segment, respectively, after [11]. (1) Shear fracture, (2) transensional fracture, (3) spreading axis.

of the crustal layer as a result of recurrent intrusions at the spreading axis. This model is considered in [3, 4, 9]. It has been shown that the thermal status of the lithosphere in the rift zone depends on the spreading rate, which controls the periodicity of intrusions during the tectonomagmatic cycle, the mantle temperature, and the intensity of magma supply determined by the thickness of the crust. In this paper, the lower boundary of the lithosphere is defined as corresponding to the solidus temperature of rocks ($T_s \approx 1150^\circ\text{C}$). The depth of this boundary varies depending on the degree of mantle heating as was accepted in the model [3].

The settings of ultraslow spreading that may result in the formation of magma chambers were tested on the basis of numerical simulation.

A model allows us to estimate the temperature distribution and variation in the degree of partial melting beneath rift zones of MORs at variable spreading rates, mantle temperatures, and thicknesses of the crust. Numerical simulation results in a thermal image of the deep structure, which shows the arrangement, shape,

and dimensions of multilevel magma sources within the crust and the subcrustal mantle immediately beneath the spreading axis and at variable distances from it.

Calculations have shown that at slow and ultraslow spreading rates (≤ 2 cm/yr) and at a frequency of the tectonomagmatic cycle that measures thousands to a few tens of thousands years, a region of focused mantle upwelling with an elevated melt concentration forms in the subcrustal mantle. Depending on the initial heating of mantle rocks, the region of focused mantle upwelling remains in the mantle at $T_m = 1100$ – 1200°C , ascends up to the crust–mantle boundary at $T_m = 1200$ – 1300°C , or even enters into the crust at $T_m > 1300^\circ\text{C}$ (Fig. 8). These temperature variations determine the specific crustal structure and thickness of the lithosphere [9]. In the first case, it is difficult to suppose that magma sources can exist within the crust (Fig. 8a), so that the spreading segments are, as a rule, amagmatic. They are characterized by a low-intensity magma supply, and serpentinized peridotites are widespread in the rift zone. In the second case, only local

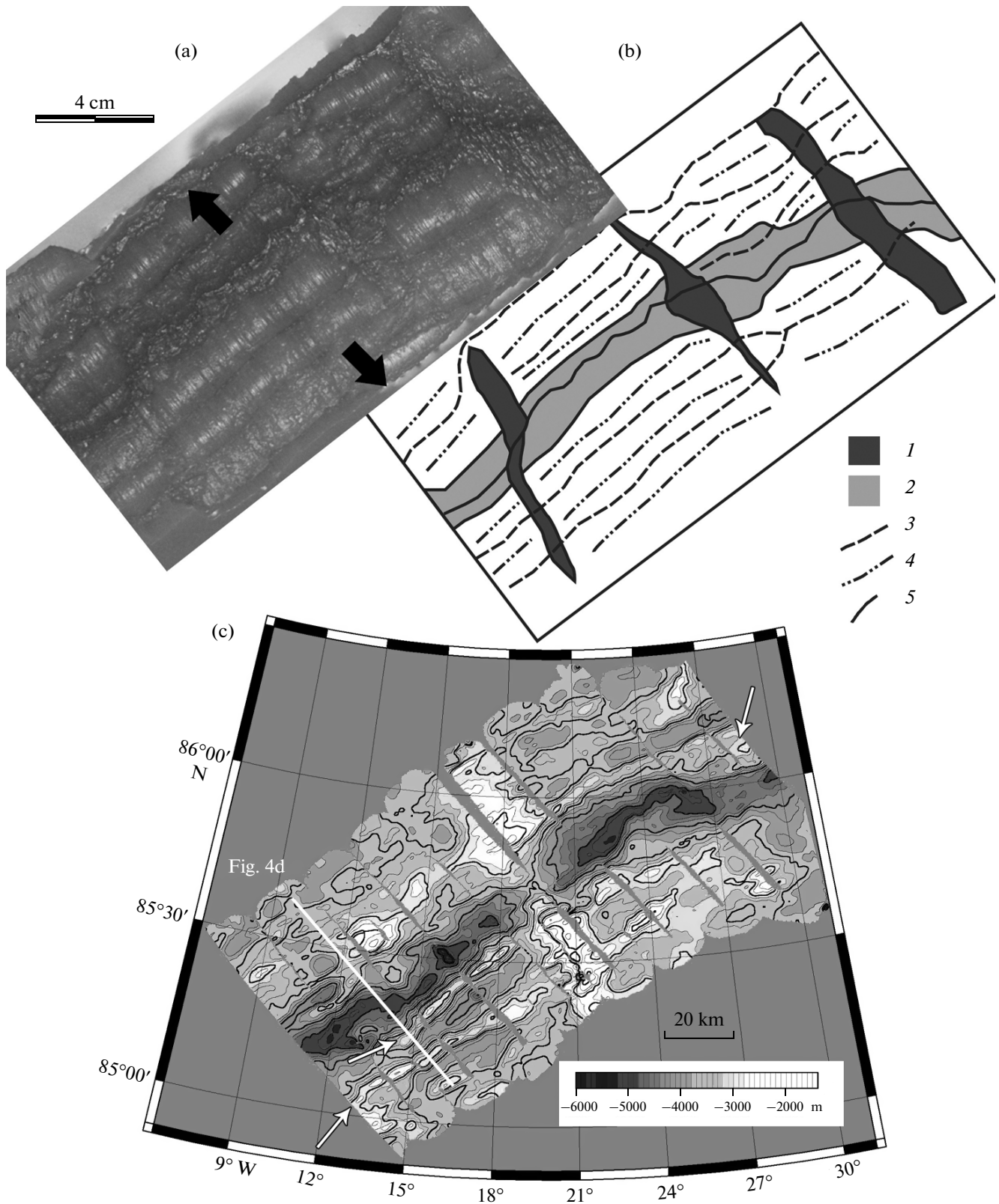


Fig. 12. Experimental results on simulation of structure-forming in rift zone structure of the Gakkel Ridge: (a) photograph of run, direction of extension shown by arrows and (b) its interpretation; (c) bathymetric map of a segment of the Gakkel Ridge, after [32]; arrows indicate large swell-shaped uplifts. (1) Fracture zones perpendicular to axis; (2) site of chaotic topography in model rift valley; (3) abandoned spreading axis; (4) axis of swell-shaped uplift; (5) spreading axis.

magma sources that cool by the end of tectonomagmatic cycle are possible (Fig. 8b). In the third case, at $T_m \sim 1350^\circ\text{C}$, stationary magma sources appear in the crust. The dimensions of local sources change depending on the mantle temperature (Figs. 8c, 8d).

The intensity of magma supply and the crust thickness as its quantitative measure are important additional parameters that exert a substantial influence on the formation of magma sources and the thermal structure of the axial zone. Estimation of the influence of the crust thickness on the formation of crustal and upper mantle magma sources has shown that in the case of a highly heated mantle ($T \geq 1350^\circ\text{C}$) and a crust 7–13 km thick, axial magma chambers are formed at the level of the middle crust at a depth of 3–7 km (Fig. 9a). In contrast to short-living axial magma chambers formed at the same mantle temperature and spreading rate, but at a lesser thickness of the crust, the crustal magma chambers are stationary and their lifetime covers several magmatic cycles (tens–hundreds of thousand years and longer). The estimates have shown that the crustal magma chambers become well expressed and stable at the crustal thickness greater than 8–10 km. An increase in thickness of more than 12 km does not exert a substantial effect on the shape and morphology of magmatic chambers. In the case of ultraslow spreading, such thick crust is known only in areas where the mantle plumes affect spreading. The Reykjanes and Kolbeinsey ridges forming under the influence of the Iceland plume represent such examples. In most cases, the thickness of crust in the rift zones of ultraslow ridges is much less than the average value of 6–7 km.

As was shown above, the variation in the crust thickness and mantle temperature along the strike of the Reykjanes Ridge leads to favorable conditions for the formation of stationary crustal magma chambers in the northern province of this ridge, whereas in the southern province, the magmatic sources are local and short-living. The variable thermal regime along the rift zone of the Reykjanes Ridge results in changes of axial morphology and strength of the axial and off-axial lithosphere [10].

Numerical estimates of strength variation in the rocks of the young oceanic lithosphere along the strike of rift zones in the ultraslow ridges make it possible to determine localization of weak zones in the lithosphere at various degrees of mantle heating and crust thickness. These estimates are based on rheological laws that relate elastic and viscous–plastic deformations of the oceanic lithosphere to the stresses measured in experiments on the deformation of wet and dry dolerite and dunite [3, 4, 28, 45].

The distribution of strength of the oceanic lithosphere with depth and distance from the ridge axis calculated in the thermal model of rift zones with allowance for the formation of axial magma sources confirmed the fact that isotherm of $T \approx 700^\circ\text{C}$ controls, in a first approximation, the transition from elastic to viscous–plastic deformation (Fig. 9). The brittle layer

located above this geotherm reaches 1.5–1.7 km in thickness near the ridge axis depending on mantle heating ($T = 1350\text{--}1380^\circ\text{C}$) and the occurrence of crustal magma chambers. Note that at a mean mantle temperature of $T = 1250^\circ\text{C}$, the thickness of this layer reaches 3 km at the axis and gradually becomes greater with increase of distance from the axis. A weak layer with viscous–plastic deformation of rocks is distinctly contoured below the isotherm of $T \approx 700^\circ\text{C}$. Under this weak layer, a zone of elastic deformation appears again in the lower crust or the mantle. Depending on the crust thickness, the subsiding isotherm of 700°C reaches a roof of the mantle at a different distance from the axis depending on the crustal thickness.

The simulation shows that even at the normal thickness of the crust (6–7 km) the layer of elastic deformation appears in the mantle only at a distance of about 10 km away from the ridge axis (Fig. 9b₁). For a thicker crust and a more heated mantle typical of magmatic segments, the brittle layer in the axial zone becomes thinner and strength at the crust–mantle boundary remains practically unchanged (Figs. 9b₂, 9b₃). In these cases, the oceanic lithosphere is composed of two relatively strong brittle layers parted by a relatively thin and weak viscous–plastic layer.

At the mantle temperature below $T < 1350^\circ\text{C}$, a zone of elastic deformation in the ultraslow spreading ridges, e.g., in the southern segment of the Reykjanes Ridge, begins immediately from the ridge axis, and the off-axis topography along the slopes of spreading ridges is formed by the blocks upthrown along the faults in the process of extension of the relatively strong lithosphere. Thus, a relatively great thickness of the effectively elastic axial lithosphere in the slow-spreading MORs is indicated by significantly large sleep of reverse faults and, as a consequence, in the advanced dissection of topography in the rift zone than in a less strong and thin axial lithosphere and with a more heated mantle.

Thus, the results of numerical simulation of ridges with ultraslow spreading rates support the model of crustal accretion, in which relatively cold amagmatic segments with a thin crust and thick and strong lithosphere give way to magmatic segments with increasing magma supply and a highly heated mantle, in combination with a thickened crust and thinner and weaker lithosphere.

EXPERIMENTAL MODELLING OF STRUCTURE-FORMING PROCESSES UNDER THE SETTINGS OF ULTRASLOW SPREADING

In order to explain the observed topography and specific structure-forming processes in the considered spreading ridges we performed the experimental simulation taking into account their kinematic features and structure. The technique of the experiments and the results were published in [6, 24, 49, 62].

In modeling the structure-forming processes at the Reykjanes Ridge, an oblique weak zone oriented at an angle of 65° to the direction of extension was introduced to simulate separately its three provinces, which differ in morphology, thickness of the brittle layer of the lithosphere, and the width of the rift zone. The fractures formed by the extension of the modeling lithosphere were S-shaped and en echelon arranged. While propagating, they occupied the most orthogonal direction relative to the direction of extension, then stretched, and finally merged (Fig. 10).

The runs showed a difference in morphology of fractures depending on the thickness of the brittle layer of the lithosphere. The degree of their segmentation increases with increasing of its thickness. Under real conditions, a melt uses these fractures to ascend to the surface, where axial volcanic rises are formed along fractures. These rises become shorter southward with increasing thickness of the brittle lithospheric layer and decreasing width of the rift zone (Figs. 10b, 10c).

Due to the obliquity of the weakened zone, the echelons of S-shaped fractures that formed in the experiments shifted relative to one another toward obliquity. Their strike was oriented at an angle of 70° – 80° to the extension axis (Fig. 10); i.e., they tended to localize more orthogonally to the direction of extension as compared with the general strike of the weakened and thinned rift zone.

Thus, the morphology of the rift zone of the Reykjanes Ridge and the character of structure-forming processes related to the failure of the brittle lithosphere change with distance from Iceland. These variations are caused, to a great extent, by variable heating of the mantle (width of the heated zone), as well as by the occurrence or absence of short-living magma sources and the thickness of the effectively elastic layer of the axial lithosphere [10].

The experiments on simulation of structure formation at the Knipovich Ridge were carried out for the entire transitional zone between the Mohs and Gakkel ridges (angle $\alpha = 33^\circ$) and for the northern and southern segments of the Knipovich Ridge with characteristic angles α of 50° and 40° . The experiments have shown that the angle between the weakened zone and the direction of extension are crucial factors that determine character of segmentation. At an obliquity of 10° – 20° , pure shears are the predominant structures. At an obliquity of 20° – 25° , a system of transtensional fractures with a prevalent shear component is observed. At an angle of 25° – 35° , shears and transtensional fractures are approximately equal in length. At an angle larger than 35° , transtensional fractures become prevalent; however, a significant shear component still remains up to an angle of 50° [12, 13].

In the Knipovich Ridge model, “pull-apart” basins were formed. These are short basins oriented either orthogonal or at an angle of 10° – 20° to the extension vector and are related to shears and transtensional fractures (Fig. 11). The segmentation of the entire sys-

tem was unstable with numerous jumps and abandonments of particular elements of the spreading axis.

It should be noted that no shears similar to those observed in the experiments were indicated during a detailed study of rift zone at the Knipovich Ridge [11, 33, 54]. However, to a first approximation, the fracture pattern of the experimental transitional zone of the Knipovich Ridge with alternation of orthogonal tension cracks and transtensional fractures nearly parallel to extension satisfactory reproduces the structure of rift zone at this ridge. Nevertheless, the natural stress field of the rift zone is much more complicated and requires more complex models for its reproduction in experiments.

The setup of the experiments reproducing the structure-forming processes at the Gakkel Ridge is based on an orthogonal and very slow extension with a narrow heating zone and a relatively thick axial lithosphere [12]. The initial failure was expressed in a practically rectilinear fracture system. The fractures are occasionally curved and overlapped; they were inherited by the structure of the growing crust throughout the experiment (Figs. 12a, 12b) and expressed in the topography of the model as depressions 1.0–1.5 cm deep. Under natural conditions, the inherited fault zones could have been the areas where large volcanic–plutonic uplifts would form.

A new crust forms with the emplacement of large swell-shaped uplifts, the width of which reached in the experiments 2.0–2.5 cm and the elevation above the bottom of the rift valley was 2–3 cm (Figs. 12a, 12b).

DISCUSSION

Geodynamic Factors Determining Tectonic Structure and Magmatism of Ultraslow Spreading Ridges

The tectonic and magmatic processes that develop under settings of ultraslow spreading are primarily controlled by relatively low heating of the mantle, low intensity of magma supply, and kinematics of orthogonal or oblique spreading. These factors result in a reduced thickness of the crust and increased thickness of the brittle lithospheric layer with an occurrence of widespread serpentinites and Na-TOR tholeiites derived from the shallow-seated sources, which are not reported in the fast-spreading ridges. Specific conditions that complicate accretion of the crust and determine the unique character of the structure of a particular ridge are superposed on the general geodynamic background of ultraslow spreading. These conditions may be related to the effects of hotspots and mantle plumes (Reykjanes and Kolbeinsey ridges, western and central segments of the SWIR), which contribute to heating of the mantle and intensify magma supply and development of TOR-1 magmatism. The neighboring continents affect the intensity of sedimentation in the rift zone (Knipovich and Gakkel ridges). The specific evolution history of some provinces in spreading ridges, e.g., the Kolbeinsey

Ridge and SWIR, should also be mentioned as a significant superposed factor. The analysis of the geological and geophysical data and the results of numerical and physical simulations allowed us to reveal the main factors that control structure-forming processes and magmatic activity. For the Reykjanes and Kolbeinsey ridges, these factors are represented by variable thickness of the crust, relative thickness of its brittle and plastic layers, width of the rift zone, increase in the intensity of magma supply and volcanic activity as approaching the Iceland thermal anomaly, and obliquity of spreading. For the Knipovich Ridge, the main factors are its formation in the transitional zone between the Mohns and Gakkel ridges under settings of interacting shearing and extension and numerous rearrangements of spreading; deviation from orthogonal spreading; and the occurrence of Barents Sea shelf and Spitsbergen as a structural and compositional barrier of the continental lithosphere. For the Mohns Ridge, the superposed factors comprise oblique spreading under conditions of the thick and cold lithosphere and the narrow stable rift zone. The Gakkel Ridge and the SWIR are distinguished by the slowest spreading rate combined with variable heating of the mantle and geometry of spreading along the strike of these ridges. The relationships between endogenic topography-forming processes vary along the strike of these ridges. With predominance of the tectonic factor, magmatic (hot spreading) and metamorphic (serpentinization of mantle rocks, cold or dry spreading) factors are locally important.

The kinematics and geometry of spreading have a direct impact on segmentation of spreading ridges. In general, four types of the segmentation of the rift zone are recognized for ultraslow spreading (Figs. 13, 2): (1) segmentation of orthogonal spreading (Figs. 13c, 13d); (2) segmentation of oblique spreading (Figs. 13a, 13b, 13e, 13f); (3) segmentation of oblique spreading under conditions of a highly heated lithosphere (Fig. 2b); and (4) segmentation of oblique spreading under the condition of a complexly built transitional zone between two other spreading ridges (Fig. 3).

The first type is characteristic of the western and central segments of the Gakkel Ridge; the Kolbeinsey Ridge; and provinces A, C, D and sites of provinces E and F of the SWIR (33–38% of the total length of all ridges under consideration). The second type is inherent to the Reykjanes and Mohns ridges; the eastern segment of the Gakkel Ridge; province B and most segments of provinces E and F in the SWIR (≈ 50 – 55% of the total length of all ultraslow spreading ridges under consideration). The third type is exemplified in the Gakkel Ridge and some sites of province D in the SWIR and characterized by echelons of S-shaped fractures as conduits for axial volcanoes (≈ 5 – 8% of the total length of all ultraslow spreading ridges under consideration).

The fourth type, which is noted in the transitional zone between the Mohns and Gakkel ridges (Knipov-

ich Ridge, Molloy Ridge, and Lena Trough), amounts to 11–15% of the total length of all spreading centers under consideration. Spreading is characterized by the oblique mechanism. Thus, oblique extension is generally typical of ultraslow spreading.

Tectonotypes of Ultraslow Spreading Ridges

Slow-, medium-, fast-, and ultrafast-spreading ridges are represented by specific tectonotypes. These are the MAR, SEIR, the northern and southern branches of the EPR. Concerning ultraslow-spreading ridges, it is difficult to choose a universal tectonotype that would illustrate their common structural features.

The comparative analysis of morphology, tectonic structure and kinematics of rift zones of ultraslow-spreading ridges allowed us to recognize several tectonic types.

(1) The spreading ridges that develop under effect of a hotspot (the Reykjanes and Kolbeinsey ridges; provinces A and D of the SWIR). The predominance of TOR-1 magmatism often with enriched geochemical signatures is typical.

(2) The spreading ridges with nearly orthogonal extension, which are undisturbed by TFZs.

(3) The spreading ridges with the least intensity of magma supply associated with highly oblique spreading and/or relatively cold mantle (the central amagmatic segment of the Gakkel Ridge; provinces B and F in the SWIR). The absence of magmatism or occurrence of the Na-TOR-type basalts related to a shallow-seated source is typical.

(4) Spreading ridges that are characterized by a stable narrow rift zone (Mohns Ridge). TOR-2 igneous rocks with depleted or asthenospheric characteristics are inherent to this type.

(5) Young spreading ridges that formed under the settings of extension with a significant shear component are localized in the transitional zone between other ridges (the Knipovich Ridge and the Lena Trough). Na-TOR tholeiitic magmatism with enriched geochemical characteristics is typical.

The first type is distinguished by significant variation in the mantle temperature along the strike of the ridge, which controls variation in thickness of the brittle layer and the width of heating zone as approaching the thermal anomaly. This variation is reflected in the change of axial morphology and structural segmentation of ridge that become different from typical slow spreading settings and become more similar to the fast spreading settings. The length of axial volcanic ranges increases, and their elevation and offsets decrease in the same direction. The melt pours out from separate volcanic vents. TFZs are formed under the asymmetric effect of the thermal anomaly. Spreading develops in both orthogonal and oblique regimes. The crust thickness is greater than the mean value characteristic of slow spreading and increases as approaching the

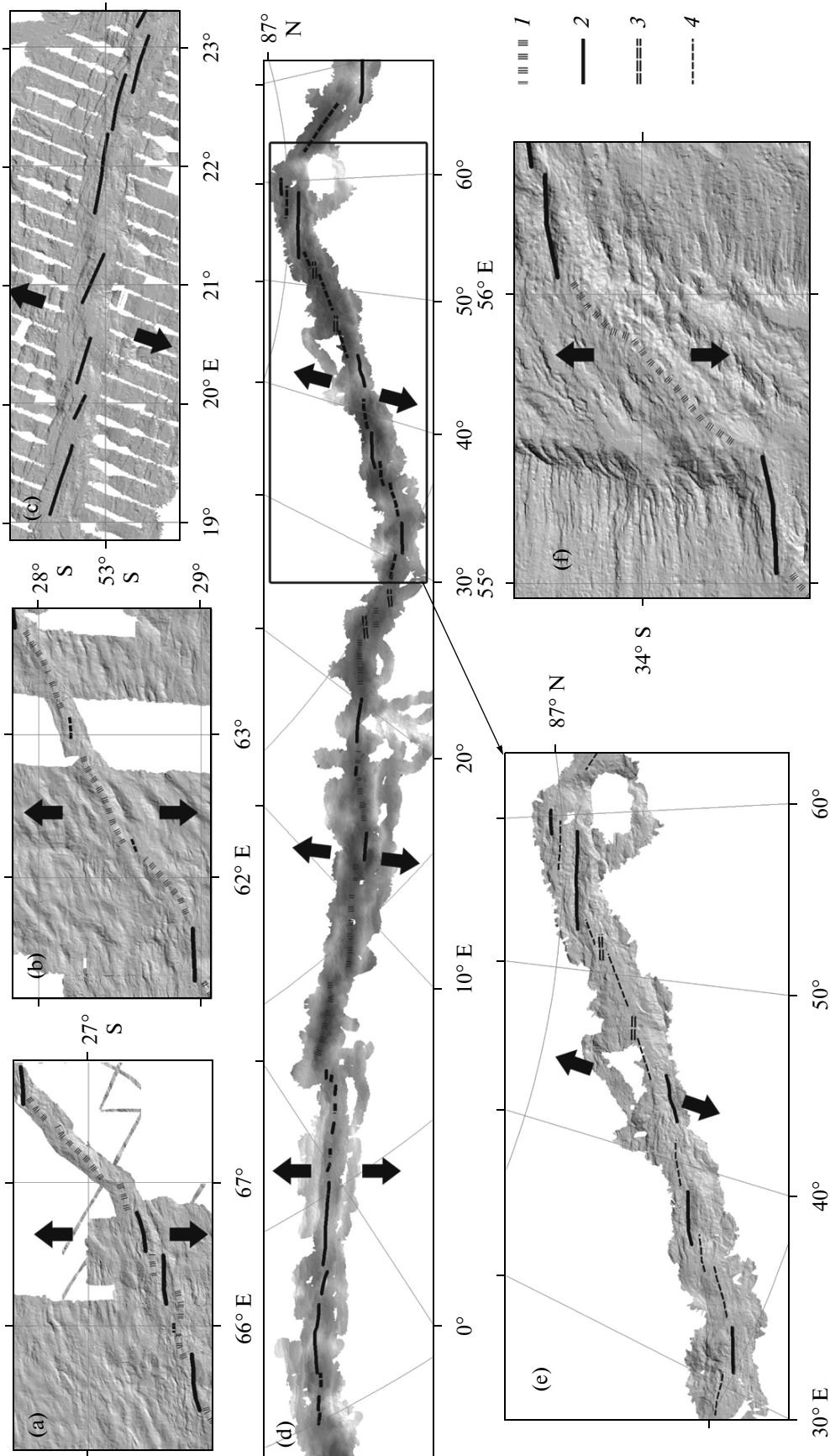


Fig. 13. Geometric types of spreading and their effect on segmentation of rift zones in spreading ridges: (a, b) sites in province F of SWIR, after [29]; (c) site in province C of the SWIR with orthogonal spreading, after [39]; (d) western volcanic segment (3° W–3° E), central amagmatic segment (3°–30° E), and eastern volcanic segment (to the east of 30° E) of the Gakkel Ridge, after [50]; (e) site of eastern volcanic segment of Gakkel Ridge, after [59]; (f) a site of province E in SWIR, after [59]. (1) amagmatic and (2) magmatic segments; (3) short-living reduced volcanic centers; (4) amagmatic segment with a thin cover of basalts.

thermal anomaly. The thickness of the brittle layer is reduced in the same direction.

The second type is characterized by extended and high axial volcanic rises in the rift valley, which are not disturbed by large offsets. The morphometric parameters of the off-axis blocky topography, and the morphology of axial volcanic ranges and separated sites of the rift zone are comparable with similar parameters of the slow-spreading MAR. The crust thickness approximately coincides with the thickness characteristic of slow spreading or is somewhat thinner.

The third, fourth, and fifth types are characterized by unique segmentation of amagmatic and magmatic segments. The amagmatic segments are oriented both obliquely and nearly orthogonal with respect to extension axis. The depth of bottom reaches 4.5–5.7 km therein. The volcanic activity is either reduced or completely absent. Peridotites are largely dredged from the bottom of rift valley; basalts are much less abundant or lacking altogether. Volcanic centers occur only sporadically. The off-axis zones look like swell-shaped uplifts. The crustal thickness is 0–3 km. The magmatic segments occupy a lesser part of the spreading ridges. They are oriented nearly orthogonal relative to the extension axis and are centers of focused magmatism. The crust is 3–7 km in thickness. In the axial parts of the ridges, volcanic rises with extended off-axis trails in the form of asymmetric blocky uplifts correspond to the magmatic segments. The depth of the bottom is 1.5–3.0 km.

The ultraslow ridges of the fifth type are shear–transensional systems localized between two neighboring spreading ridges, e.g., the transitional zone between the Mohns and Gakkal ridges. They are characterized by a complex combination of amagmatic segments variable in length and short magmatic segments, which often correspond to pull-apart structures. The geological–geophysical and geomorphic structure of the segments depends on their orientation relative to the direction of plate divergence and on the relationships between the shear and pull-apart elements in their kinematics.

Dick et al. [36] suggested that the extreme case of dry ultraslow spreading is noted at an effective spreading rate lower than 13 mm/yr. This type of spreading is distinguished by the following attributes: (i) a minimum number of volcanic edifices, most of which are localized at the walls of the axial valley [31, 65]; (ii) a reduced crustal section—the thickness of the second layer is 1–2 km and the third layer is completely absent [41–43]; a maximum depth of the rift valley reaching 4.5–5.7 km; (iii) swell-shaped uplifts on the ridge's flanks [29, 30]; and (iv) widespread serpentinized peridotites [30, 36, 50, 60]. Indeed, these features characterize the central amagmatic segments of the Gakkal Ridge, the Lena Trough, and some sites of the B and F provinces in the SWIR. At the same time, they are poorly expressed in the eastern volcanic segment of the Gakkal Ridge and in province E of the SWIR with

a spreading rate of <13 mm/yr. The amount of the dredged basalts increases here; the depth of the bottom does not reach 4.0–4.5 km, and the swell-shaped uplifts are poorly expressed. Features characteristic of extreme dry ultraslow spreading were not established at the Knipovich Ridge, where the axial depth does not exceed 3.5–3.7 km and off-axis swell-shaped uplifts were noted only in the junction zone of the Mohns and Knipovich ridges. This implies that the temperature of the underlying mantle, distance from continent, geological history, and other factors affect the character of the topography and segmentation in addition to the geometry and kinematics of spreading.

CONCLUSIONS

The morphological and geological–geophysical characteristics of the considered ultraslow spreading ridges and the simulation results allowed us to establish the main structure-forming factors that act in their rift zones. As concerns the Reykjanes Ridge, the effect of the Iceland thermal anomaly under conditions of oblique spreading is crucial. As a result, the mantle temperature, the volume of magmatic melts, the thickness of the crust, and of the brittle crustal layer vary with distance from Iceland along the strike of this ridge. Three provinces differ in the morphology of rift zone and its structural segmentation. Experiments with different thicknesses of the brittle layer in the model lithosphere and width of the heating zone yielded the patterns of segmentation of axial fractures close to the natural structure.

The structure-forming processes at the Kolbeinsey Ridge is amenable to similar relationships. The topography of this ridge is more dissected and contrasting, spreading is nearly orthogonal, and the crust thickness is less than in the rift zone of the Reykjanes Ridge, indicating the asymmetric influence of the Iceland plume. Owing to nearly orthogonal spreading, a system of poorly echeloned volcanic ranges is formed in the rift zone; these ranges are higher and longer than in the Reykjanes Ridge. A system of extended and poorly echeloned fractures, the morphology of which varies depending on the width of heating zone and the thickness of the brittle crustal layer, was simulated in the laboratory [12].

At the Mohns Ridge, the divergence stably develops under the settings of oblique spreading within a narrow deformation zone without rupture of continuity and transform offsets. This gave rise to the formation of a stable system of accretionary segments oriented nearly orthogonal to the extension axis and separated by shear and transensional zones near-parallel to the extension, which accommodated tensile stresses.

At the Knipovich Ridge, the structure-forming processes are affected by the young age and instability of the plate boundary, which is currently forming. The shear and tensile stresses are competing in the extension kinematics of each segment of this ridge.

Depending on their relationships, the geomorphic appearance of the rift valley changes in each segment. Physical simulation has shown that owing to even insignificant variation in the orientation of ridge segments, the structure of the rift zone changes from shears to transtensional fractures with the formation of pull-apart basins connected by shears. The pull-apart structure is expressed in topography as volcanic uplifts orthogonal with respect to extension axis, whereas shear deformation, as troughs and slightly elongated basins with reduced volcanic activity.

The Gakkel Ridge and the SWIR are distinguished by the lowest spreading rate and a significant thickness of the lithosphere. The degree of mantle heating and geometry of spreading vary along the strike of the ridges. The relationships between endogenic processes also change along the strike. A prevalent tectonic factor is combined with locally developed magmatic and metamorphic processes.

ACKNOWLEDGMENTS

We thank K.A. Skripko for his assistance in preparation of the manuscript and the reviewers for their constructive criticism.

This study was supported by the Russian Foundation for Basic Research (project nos. 12-05-00528 and 12-05-00582) and the Ministry of Education and Science of the Russian Federation (federal target program "Human Resources in Science and Education for Innovative Russia").

REFERENCES

1. G. P. Avetisov, "Geodynamics of the Submarine Knipovich Ridge (Norwegian–Greenland Basin)," in *Geological and Geophysical Characteristics of the Arctic Lithosphere* (VNIIOkeangeologiya, St. Petersburg, 1998), Issue 2, pp. 46–57 [in Russian].
2. E. V. Verzhbitskii, M. V. Kononov, A. F. Byakov, and O. V. Grinberg, "Genesis of the Lithosphere of the Iceland Region (North Atlantic) According to Geophysical Data," *Oceanology* **49** (2), 228–241 (2009).
3. Yu. I. Galushkin, E. P. Dubinin, and A. A. Sveshnikov, "A Nonstationary Model of the Thermal Regime of Axial Zones of Mid-Ocean Ridges: Formation of Crustal and Mantle Magma Chambers," *Izv. Physics Solid Earth* **43** (2), 130–147 (2007).
4. Yu. I. Galushkin, E. P. Dubinin, and A. A. Sveshnikov, "Rheological Layering of the Oceanic Lithosphere in Rift Zones of Mid-Oceanic Ridges," *Dokl. Earth Sci.* **418** (1), 114–117 (2008).
5. V. Yu. Glebovitsky, V. D. Kaminsky, A. N. Minakov, et al., "Formation of the Eurasia Basin in the Arctic Ocean as Inferred from Geohistorical Analysis of the Anomalous Magnetic Field," *Geotectonics* **40** (4), 263–281 (2006).
6. A. L. Grokhol'sky and E. P. Dubinin, "Experimental Modeling of Structure-Forming Deformations in Rift Zones of Mid-Ocean Ridges," *Geotectonics* **40** (1), 64–80 (2006).
7. L. V. Dmitriev, A. V. Sobolev, and N. M. Sushchevskaya, "Formation Conditions of Primary Melt of Oceanic Tholeiites and Variations of Its Composition," *Geokhimiya* **17** (2), 163–175 (1979).
8. E. P. Dubinin and S. A. Ushakov, *Oceanic Rifting* (GEOS, Moscow, 2001) [in Russian].
9. E. P. Dubinin, Yu. I. Galushkin, and A. A. Sveshnikov, "A Model of Oceanic Crust Accretion and Geodynamic Implications," in *Life of the Earth* (Moscow State Univ., Moscow, 2010), Issue 32, 53–82 [in Russian].
10. E. P. Dubinin, A. L. Grokhol'sky, A. V. Kokhan, and A. A. Sveshnikov, "Thermal and Rheological State of the Lithosphere and Specific Features of Structuring in the Rift Zone of the Reykjanes Ridge (from the Results of Numerical and Experimental Modeling)," *Izv. Physics Solid Earth* **47** (7), 586–599 (2011).
11. A. V. Zaionchek, H. Brekke, S. Yu. Sokolov, et al., "Structure of Continent–Ocean Transition Zone in the Northwestern Framework of the Barents Sea from the Results of 24, 25 and 26 Cruises of the R/V *Akademik Nikolai Strakhov*, 2006–2009," in *Structure and Evolution History of the Lithosphere: Contribution of Russia to the International Polar Year* (Paulsen, Moscow, 2010), Vol. 4, pp. 111–157 [in Russian].
12. A. V. Kokhan, E. P. Dubinin, and A. L. Grokhol'sky, "Geodynamic Features of Structure-Forming Processes in Spreading Ridges of Arctica and Polar Atlantic," *Vestnik KRAUNTs, Nauki o Zemle*, No. 1, 59–77 (2012).
13. A. V. Kokhan, E. P. Dubinin, A. L. Grokhol'sky, and A. S. Abramova, "Kinematics and Characteristic Features of the Morphostructural Segmentation of the Knipovich Ridge," *Oceanology* **52** (5), 688–699 (2012).
14. S. A. Merkur'ev, Ch. De Metts, and N. I. Gurevich, "Geodynamic Evolution of Crust Accretion at the Axis of the Reykjanes Ridge, Atlantic Ocean," *Geotectonics* **43** (3), 194–207 (2009).
15. A. A. Peyve and N. P. Chamov, "Basic Tectonic Features of the Knipovich Ridge (North Atlantic) and Its Neotectonic Evolution," *Geotectonics* **42** (1), 31–47 (2008).
16. A. A. Peyve, "Accretion of Oceanic Crust under Conditions of Oblique Spreading," *Geotectonics* **43** (2), 87–99 (2009).
17. Yu. M. Pushcharovsky, "Geodynamic Variations in Ocean-Floor Spreading with Reference to the Atlantic Ocean," *Geotectonics* **37** (4), 261–270 (2003).
18. I. M. Sborshchikov and M. V. Rudenko, "Structure of Rift Zone of the Reykjanes Ridge and the Iceland Thermal Anomaly," *Geotektonika* **19** (2), 88–103 (1985).
19. S. Yu. Sokolov, "Tectonic Evolution of the Knipovich Ridge Based on the Anomalous Magnetic Field," *Dokl. Akad. Nauk* **437** (3), 343–348 (2011).
20. N. M. Sushchevskaya, L. V. Dmitriev, and A. V. Sobolev, "Petrochemical Criteria of Classification of Quenched Glasses of Oceanic Tholeiites," *Dokl. Akad. Nauk SSSR* **268** (6), 953–961 (1983).
21. N. M. Sushchevskaya, T. I. Tsekhnova, E. P. Dubinin, E. G. Mirilin, and N. N. Kononkova, "Formation of

- Oceanic Crust in Mid-Ocean Ridges of the Indian Ocean," *Geochem. Int.* **34** (10), 869–880 (1996).
22. N. M. Sushchevskaya, G. A. Cherkashov, B. V. Baranov, K. Tomaki, H. Sato, H. Nguen, B. V. Belyatsky, and T. I. Tsekhonya, "Tholeiitic Magmatism of an Ultraslow Spreading Environment: An Example from the Knipovich Ridge, North Atlantic," *Geochem. Int.*, **43** (3), 222–241 (2005).
 23. N. M. Sushchevskaya, V. S. Kamenetsky, B. V. Belyatsky, and A. V. Artamonov, "Geochemical Evolution of Basaltic Magmatism in the Indian Ocean," *Geochem. Int.*, (in press).
 24. A. I. Shemenda, "Simulation Criteria in Mechanical Modeling of Tectonic Processes," *Geol. Geofiz.* **24** (10), 10–19 (1983).
 25. E. V. Shipilov, "Generations of Spreading Basins and Stages of Breakdown of Wegener's Pangea in the Geodynamic Evolution of the Arctic Ocean," *Geotectonics* **42** (2), 105–124 (2008).
 26. B. Appelgate, Geophysical Investigations of the Reykjanes Ridge and Kolbeinsey Ridge Seafloor Spreading Centers, *PhD Thesis*, Univ. Hawaii, 1995, 86 p.
 27. B. Appelgate and A. N. Shor, "The Northern Mid-Atlantic and Reykjanes Ridges: Spreading Center Morphology between 55°50' N and 63°00' N," *J. Geophys. Res.* **99**, 17935–17956 (1994).
 28. G. Bassi and J. Bonnin, "Rheological Modeling and Deformation Instability of Lithosphere Under Extension—II. Depth-Dependent Rheology," *Geophys. J.* **94**, 559–565 (1988).
 29. M. Cannat, D. Sauter, V. Mendel, et al., "Modes of Seafloor Generation at a Melt-Poor Ultraslow-Spreading Ridge," *Geology* **34** (7), 605–608 (2006).
 30. M. Cannat, D. Sauter, A. Bezous, et al., "Spreading Rate, Spreading Obliquity and Melt Supply at the Ultraslow-Spreading Southwest Indian Ridge," *Geochem. Geophys. Geosyst.* **9**, (2008). doi: 10.1029/2007GC001676
 31. J. R. Cochran, "Seamount Volcanism along the Gakkel Ridge, Arctic Ocean," *Geophys. J. Int.* **174**, 1153–1173 (2008).
 32. J. R. Cochran, G. J. Kurras, M. H. Edwards, and B. Coakley, "The Gakkel Ridge: Bathymetry, Gravity Anomalies and Crustal Accretion at Extremely Slow Spreading Rates," *J. Geophys. Res.* **108**, 2116–2137 (2003).
 33. K. Crane, H. Doss, P. Vogt, et al., "The Role of the Spitzbergen Shear Zone in Determining Morphology, Segmentation and Evolution of the Knipovich Ridge," *Mar. Geophys. Res.* **22**, 153–205 (2001).
 34. D. Curewitz, K. Okino, M. Asada, et al., "Structural Analysis of Fault Populations along the Oblique, Ultra-Slow Spreading Knipovich Ridge, North Atlantic Ocean, 74°30' N–77°50' N," *J. Struct. Geol.* **32**, 727–740 (2010).
 35. C. DeMets, R. Gordon, and D. Argus, "Geologically Current Plate Motions," *Geophys. J. Int.* **181**, 1–80 (2010).
 36. H. Dick, J. Lin, and H. Schouten, "An Ultra-Slow Class of Spreading Ridge," *Nature* **426**, 405–412 (2003).
 37. CEBCO_08 Grid, Ver. 20100927, <http://www.gebco.net>
 38. L. Geli, V. Renard, and C. Rommevaux, "Ocean Crust Formation Processes at Very Slow Spreading Centers: A Model for the Mohs Ridge, near 72° N, Based on Magnetic, Gravity, and Seismic Data," *J. Geophys. Res.* **99**, 2995–3013 (1994).
 39. N. Grindlay and J. Madsen, et al., "A Different Pattern of Ridge Segmentation and Mantle Bouger Gravity Anomalies along the Ultra-Slow Spreading Southwest Indian Ridge (15°30' E to 25° E)," *Earth Planet. Sci. Lett.* **161**, 243–255 (1998).
 40. E. E. Hooft, B. Brandstottir, R. Mjelde, et al., "Asymmetric Plume–Ridge Interaction around Iceland: The Kolbeinsey Ridge Iceland Seismic Experiment," *Geochem. Geophys. Geosyst.* **7**, 1–26 (2006).
 41. W. Jokat, O. Ritzmann, M. Schmidt-Aursch, et al., "Geophysical Evidence for Reduced Melt Production on the Arctic Ultraslow Gakkel Mid-Ocean Ridge," *Nature* **423**, 962–965 (2003).
 42. W. Jokat and M. Schmidt-Aursch, "Geophysical Characteristics of the Ultraslow Spreading Gakkel Ridge, Arctic Ocean," *Geophys. J. Int.* **168**, 983–998.
 43. A. Kandilarov, R. Mjelde, K. Okino, and Y. Murai, "Crustal Structure of the Ultra-Slow Spreading Knipovich Ridge, North Atlantic, along a Presumed Amagmatic Portion of Oceanic Crustal Formation," *Mar. Geophys. Res.* **29**, 109–134 (2008).
 44. J. A. Keeton, R. C. Searle, B. Parsons, et al., "Bathymetry of the Reykjanes Ridge," *Mar. Geophys. Res.* **19**, 55–64 (1997).
 45. S. H. Kirby, "Rheology of the Lithosphere," *Rev. Geophys. Space Phys.* **21**, 1458–1487 (1983).
 46. E. M. Klein and C. H. Langmuir, "Global Correlations of Ocean Ridge Basalt Chemistry with Axial Depth and Crustal Thickness," *J. Geophys. Res.* **92** (B4), 8089–8115 (1987).
 47. F. Klingelhofer, L. Geli, L. Matias, et al., "Geophysical and Geochemical Constraints on Crustal Accretion on the Very-Slow Spreading Mohs Ridge," *Geophys. Res. Lett.* **27** (10), 1547–1550 (2000).
 48. S. Kodaira, R. Mjelde, K. Gunarsson, et al., "Crustal Structure of the Kolbeinsey Ridge, North Atlantic, Obtained by Use of Ocean Bottom Seismographs," *J. Geophys. Res.* **102**, 3131–3151 (1997).
 49. B. V. Malkin and A. I. Shemenda, "Mechanism of Rifting: Consideration Based on Results of Physical Modeling and on Geological and Geophysical Data," *Tectonophysics* **199**, 193–210 (1991).
 50. P. J. Michael, C. H. Langmuir, H. J. Dick, et al., "Magmatic and Amagmatic Seafloor Generation at the Ultraslow-Spreading Gakkel Ridge, Arctic Ocean," *Nature* **423**, 956–961 (2003).
 51. R. Mjelde, T. Raum, A. J. Breivik, and J. I. Faleide, "Crustal Transect across the North Atlantic," *Mar. Geophys. Res.* **29**, 73–87 (2008). doi: 10.1007/s11001-008-9046-9
 52. B. J. Murton and L. M. Parson, "Segmentation, Volcanism and Deformation of Oblique Spreading Centers: a Quantitative Study of the Reykjanes Ridge," *Tectonophysics* **222**, 237–257 (1993).
 53. F. Nauret, J. E. Snow, E. Hellebrand, and D. Weis, "Geochemical Composition of K-Rich Lavas from the

- Lena Trough (Arctic Ocean),” *J. Petrol.* **52** (6), 1185–1206 (2011). doi: 10.1093/petrology/egr024
54. K. Okino, D. Curewitz, M. Asada, et al., “Preliminary Analysis of the Knipovich Ridge Segmentation: Influence of Focused Magmatism and Ridge Obliquity on an Ultraslow Spreading System,” *Earth Planet. Sci. Lett.* **202**, 275–288 (2002).
 55. C. Peirce and M. C. Sinha, “Life and Death of Axial Volcanic Ridges: Segmentation and Crustal Accretion at the Reykjanes Ridge,” *Earth Planet. Sci. Lett.* **274**, 112–120 (2008).
 56. D. Sandwell and W. Smith, “Global Marine Gravity from Retracked Geosat and ERS-1 Altimetry: Ridge Segmentation Versus Spreading Rate,” *J. Geophys. Res.* **114** (B01411), 1–18 (2009). doi: 10.1029/2008JB006008
 57. D. Sauter, M. Cannat, C. Meyzen, et al., “Propagation of a Melting Anomaly along the Ultraslow Southwest Indian Ridge between 46° E and 52°20' E: Interaction with Crozet Hotspot?,” *Geophys. J. Int.* **179**, 687–699 (2009).
 58. D. Sauter and M. Cannat, “The Ultraslow Spreading Southwest Indian Ridge,” in *Diversity of Hydrothermal Systems on Slow Spreading Ocean Ridges*, (AGU, Geophys. Monograph Ser., 2010), Vol. 188, pp. 153–173.
 59. R. C. Searle, J. A. Keeton, R. B. Owens, et al., “The Reykjanes Ridge: Structure and Tectonics of a Hot-Spot-Influenced, Slow-Spreading Ridge, from Multi-beam Bathymetry, Gravity and Magnetic Investigations,” *Earth Planet. Sci. Lett.* **160**, 463–478 (1998).
 60. M. Seyler, M. Cannat, and C. Mevel, “Evidence for Major-Element Heterogeneity in the Mantle Source of Abyssal Peridotites from the Southwest Indian Ridge (52° E to 68° E),” *Geochem. Geophys. Geosyst.* **4**, 1–33 (2003). doi: 10.1029/2002GC000305
 61. M. C. Sinha, S. C. Constable, C. Peirce, et al., “Magmatic Processes at Slow Spreading Ridges: Implications of the RAMESSES Experiment at 57°45' North on the Mid-Atlantic Ridge,” *Geophys. J. Int.* **135**, 731–745 (1998).
 62. A. I. Shemenda and A. L. Grocholsky, “Physical Modeling of Slow Seafloor Spreading,” *J. Geophys. Res.* **99**, 9137–9153 (1994).
 63. J. R. Smallwood and R. S. White, “Crustal Accretion at the Reykjanes Ridge, 61°–62° N,” *J. Geophys. Res.* **103**, 5185–5201 (1998).
 64. J. E. Snow, H. Feldmann, A. V. D. Handt, et al., “Petrologic and Tectonic Evolution of the Lena Trough and Western Gakkel Ridge,” in *Reports of Polar and Marine Research*, Ed. by G. Budeus, and P. Lemke (Alfred Wegener Institute for Polar and Marine Res., Bremerhaven, 2007), pp. 153–208.
 65. J. Standish and K. Sims, “Young Off-Axis Volcanism along the Ultraslow Spreading Southwest Indian Ridge,” *Nature Geoscience* **3**, 286–292 (2010).
 66. N. R. W. Weir, R. S. White, B. Brandsdottir, et al., “Crustal Structure of the Northern Reykjanes Ridge and Reykjanes Peninsula,” *J. Geophys. Res.* **106**, 6347–6368 (2001).
 67. R. S. White, T. A. Minshull, M. J. Bickle, and C. J. Robinson, “Melt Generation and Very Slow-Spreading Oceanic Ridges: Constraints from Geochemical and Geophysical Data,” *J. Petrol.* **42** (6), 1171–1196 (2001).

*Reviewer: A.A. Peyve
Translated by V. Popov*